UNIVERSITY OF CALIFORNIA

Los Angeles

Dynamic Surface Tension Effects
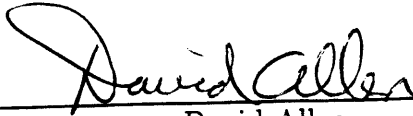
on

Oxygen Transfer

in

Activated Sludge

A dissertation submitted in partial satisfaction of the

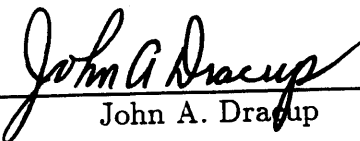requirements for the degree of

Doctor of Philosophy in Civil Engineering

By
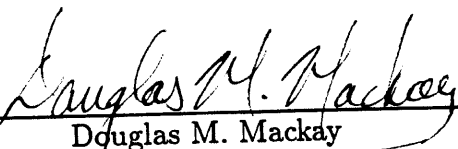
Gail Kiyomi Masutani
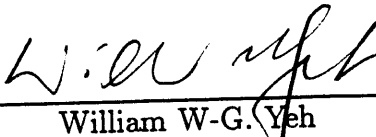
1988
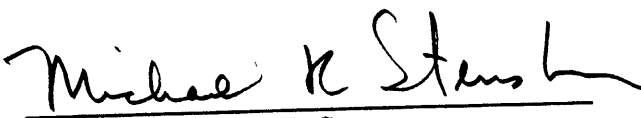
The dissertation of Gail Kiyomi Masutani is approved.

_____
David Allen

_____
John A. Dracup

_____
Douglas M. Mackay

_____
William W-G. Yeh

_____
Michael K. Stenstrom
Committee Chair

University of California, Los Angeles

1988

ii

Dedication

To Tracy   To My Parents

Contents

List of Tables

List of Figures

Acknowledgments

I would like to express my appreciation to my advisor, Professor Michael K. Stenstrom, for his guidance and encouragement throughout my academic career. It has been an honor to work with him. I would like to thank the other members of my committee: Professor Allen, Professor Dracup, Professor Mackay, and Professor Yeh.

I would like to thank former collegues: Hwang, Tran, Adam, Steve, Prasanta, Sami and Hamid for showing me the way. Special thanks to AC for your continual encouragement and just being there when I needed you. Debby, thanks for getting me in to see "the Boss", and making the graduate students' lives easier.

Finally, I would like to thank my family for their encouragement and support through the years and never giving up on me. Thanks Tracy, Mom, Dad, Brian, Cindy, Grandma, Jay, Madeline, and Jon. My Los Angeles Booster Club deserves acknowledgement also: Aunty Helen, Aunty Joyce, Uncle Mark, Robin, Ryan, the Morimotos and Mrs. Ono.

VITA

Gail Kiyomi Masutani

April 12, 1956	Born, Aiea, Hawaii
1978	B.S., Civil Engineering, University of Hawaii
1980-1981	Research Assistant, Engineering Systems Dept., University of California, Los Angeles
1981	M.S., Engineering, University of California, Los Angeles
1981-1983	Teaching Assistant, Engineering Systems Dept., University of California, Los Angeles
1984-1985	Student Engineer, Los Angeles County Engineering Facilities Div., Los Angeles, California
1985-1988	Research Assistant, Civil Engineering Dept., University of California, Los Angeles

ABSTRACT OF THE DISSERTATION

Dynamic Surface Tension Effects

on

Oxygen Transfer

in

Activated Sludge

by

Gail Kiyomi Masutani

Doctor of Philosophy in Civil Engineering

University of California, Los Angeles, 1988

Professor Michael K. Stenstrom, Chair

An important goal of environmental engineering research is to increase oxygen transfer efficiencies. Strategies include improved aeration basin geometry designs, diffuser placement and type, water depth, aerator selection, and process operating conditions. The manufacturers' shop oxygen transfer tests often fail to adequately predict operation under process conditions. This difference usually translates into substantial additional aeration costs to meet oxygen demand, and results from insufficient information regarding process water conditions.

Process water conditions for oxygen transfer are best described by mass transfer parameters. This dissertation focuses on quantifying the volumetric mass transfer coefficient, $K_L a$, and the liquid film coefficient, K_L, using dynamic surface tension (DST) measurements.

The maximum bubble pressure method was selected to measure DST because of its low cost and simplicity. DST measurements on tap water were used to calibrate the constructed measuring apparatus and served to test the accuracy of the technique. A friction factor was introduced to reconcile noisy data. Two anionic surfactants were used in two concentrations to observe their effects on diffused aeration and to characterize the DST relationship.

A mathematical model was formulated showing the DST relationship with bubble life. A slope parameter, X, and an intercept parameter, γ_∞, were estimated from the bubble life, surface tension and surfactant concentration. A high X value corresponded to increased surfactant concentration. Using X as an indicator of water quality, repeated aeration tests on surfactant solutions indicated X and K_L increased with an increasing number of experiments. This resulted from surfactant deterioration. Antifoaming agent added to foamy solutions resulted in an immediate reduction in $K_L a$, and stresses the need for their careful use when field testing.

A DST value was calculated from the model using the estimated parameters and the bubble retention time. $K_L a$ can be predicted by DST, aeration flow rate and the static surface tension measurement. The final result showed the DST parameter can estimate K_L values given the air flow rate and surfactant concentration.

Chapter 1

Introduction

Manufacturers of aeration equipment use shop oxygen transfer testing to describe the expected performance of their product. The results are reported in terms of the standard oxygen transfer rate (SOTR). The engineer attempts to extrapolate the manufacturers' performance rating to probable biological reactor results. The actual field or process results often differ from the predicted by as much as 70% because of the inherent inability to account for all the field systems' variables such as basin geometry, type of aeration technique, placement of aeration equipment, and contaminates in the liquid.

The difference between the expected and the actual performance of the system can translate to substantial additional modification costs to meet process requirements. These costs, plus time delays in achieving operational consistency, demonstrates the need for future study to better correlate the manufacturers' SOTR with field conditions.

The SOTR is related to field OTR by parameters called alpha (α), beta (β), and theta (θ). These parameters relate process water tests to clean water oxygen

transfer tests and are given by:

$$\alpha = \frac{K_L a_{PW}}{K_L a_{TW}} \tag{1}$$

$$\beta = \frac{C^*_{\infty PW}}{C^*_{\infty TW}} \tag{2}$$

$$\theta^{T-20} = \frac{K_{La}(T^\circ C)}{K_{La}(20^\circ C)} \tag{3}$$

Alpha, the ratio of the overall volumetric mass transfer coefficients, is the parameter of interest in this study. Although alpha is dependent on basin geometry, liquid properties, and aeration type, it is used to extrapolate lab results in scale-up operations and is used to predict oxygen transfer in process water. With alpha's dependence on such varied conditions, it is no wonder that its predictive performance falls short of the actual operational needs.

Another reason for the unpredictability of alpha lies in its definition through mass theory. The mass transfer coefficients used to obtain alpha factors are based on the Lewis and Whitman (1924) two film theory of steady-state gas transport through a liquid interface. In this theory, thin films of the gas and of the liquid, possessing properties different from their bulk, exist at the gas/liquid interface. Transport occurs from the bulk gas to the bulk liquid by serial molecular diffusion through both films. It is assumed that no accumulation occurs at the interface because of the turbulent transport of gas molecules away from the interface by the bulk liquid. For sparingly soluble gases, the liquid film controls diffusion and the concentration of the gas at the liquid film interface is in an equilibrium with the gas phase defined by Henry's law. The concentration of the gas in the bulk liquid is assumed to be uniform. Alpha is constructed on this steady-state system. The concentration at the interface is not constant, therefore this theory should not be applied in defining alpha.

2

Contrasting this theory are the more recent penetration and surface renewal theories in mass transport. Higbie's (1935) penetration theory proposes unsteady-state transport by assuming the liquid film is continuously replaced by "fresh" liquid from the bulk. The replacing liquid has the same gas concentration as the bulk solution. The transfer of the gas occurs by diffusion through the film at an initially high concentration gradient. Eventually the gradient decreases to the steady-state condition, indicating a significant portion of gas transfer occurs during the penetration period. In the Dankwerts (1951) surface renewal model, the residence time is no longer considered to be constant. Instead, residence time is assumed to have a normal distribution with surface age. Although these theories more closely approximate the actual transfer mechanisms, the steady-state diffusion model is used because of its simpler form for parameter estimation.

The parameter describing the mass transfer coefficient needs to better reflect actual field conditions, and the alpha factor does not. In the process water tests it especially neglects the effect of surfactant adsorption at the interface because of the steady-state assumption. It is therefore more desirable to incorporate the time-dependence nature of mass transfer into the parameter.

Static surface tension measurements have been investigated with regard to alpha values but were inconclusive (Stenstrom and Gilbert, 1981). It is thought since dynamic surface tension measurements exhibit time-dependent characteristics, thereby considering the effect of surfactants, it may be a better indicator of mass transfer.

The research goal of this dissertation is to correlate the mass transfer coefficient with a parameter that reflects the liquid properties. It is believed such a parameter can be identified by dynamic surface tension measurement. When this transfer

parameter is identified, it will better correlate the mass transfer coefficient such that the engineer will be able to better predict the field performance and realize a substantial savings in aeration costs of a wastewater treatment plant.

The objective of this dissertation is to investigate into the relationship between oxygen transfer and dynamic surface tension measurements. The literature review covers the common dynamic surface tension measuring techniques, the effects of surfactants on oxygen transfer, and aeration studies. The selected dynamic surface tension measuring technique is then used on aerated surfactant test solutions to correlate the parameter describing dynamic surface tension with oxygen transfer.

Chapter 2

Literature Review

The following literature review concentrates on the three areas of interest in this study. The first area investigates the most popular static and dynamic surface tension measuring techniques to determine the most suitable based on economics and simplicity of design. The second section gives a brief overview of surfactants and their effect on surface tension and mass transfer. The last section reviews the pertinent works in wastewater oxygen transfer.

2.1   General Surface Tension Concepts

The concept of surface tension is best explained by a few examples:

1. Surface tension was first measured using the du Nouy ring method as calculated from the force required to detach a wire ring from the horizontal liquid surface.

2. When one end of a thin capillary tube, open at both ends, is submerged into a fluid, the fluid rises to a hydrostatic height. The force pulling the fluid up

the capillary is surface tension. The weight of the fluid in the capillary tube is proportional measure of the surface tension of the fluid.

3. Similarly, liquid drops seem to have a "skin" which keeps their shape. The extent to which the "skin" holds the drop shape is dependent on its surface tension

These examples show surface tension can be represented as the work required to expand surface area per unit distance (dyne/cm) or as surface free energy (erg/cm^2) tends to a minimum. In either case, the concepts are mathematically equivalent (Harkins, 1952).

Surface tension is dependent on molecular attraction between the fluid and gas phases. The molecules in the fluid interior are attracted to one another more so than at the surface where the air molecules are less densely packed and therefore not as attracted to each other as to the water molecules. The surface molecules thus possess higher potential energies than the interior molecules (Davis and Rideal, 1961).

Surfactants are substances that, when present in low concentrations, have the ability to significantly alter the surface properties of the solvent. These compounds are generally composed of lyophobic and/or lyophilic groups. It requires less energy to bring a surfactant molecule to the surface than a water molecule because the lyophobic component of the surfactant wants to escape the surface, while the lyophyllic end of the molecule keeps the surfactant from being expelled. Since less work is required to bring molecules to the surface, surfactants accumulate at the interface and their presence decreases the work required to create new surface area.

6

The orientation of surfactant molecules at the interface has been shown to be
dependent on its molecular structure and fluid polarity. At the interface of a two
phase system, each end of the surfactant molecule orients itself such that each
lies in the more soluble phase. At an air/water interface, the nonpolar end of
surfactant molecules point in the air and polar groups tend toward the water.

2.2   Surface Tension Measurements

Surface tension measuring techniques can be categorized into two classes. The
first class is static tension measurements. Pure liquids are measured with these
devices since surface tension is constant. The second class is dynamic surface
tension measurements; many are modifications of the static models such as the
maximum bubble pressure method and the drop methods. Surfactant solutions
should be measured by these methods since surface tension is a function of time,
especially during the intitial surface ages when a sharp decrease in surface tension
is usually observed. The surface tension values approach the static value when
surface concentration of surfactants approaches equilibrium.

Before presenting a review of the various methods of surface tension measuring
techniques, surface age and surface time must be defined. Surface age, as defined
by various researchers, refers to the length of time from surface formation to some
specified time (usually until a measurement is taken). Surface time, in general, is
defined as the marking of period intervals; and is not necessarily measured from
the start of surface formation. For example, in the maximum bubble method,
surface age is the time interval from the start of the surface formation to the point
when the radius of the bubble is equal to the capillary radius. Surface time is the
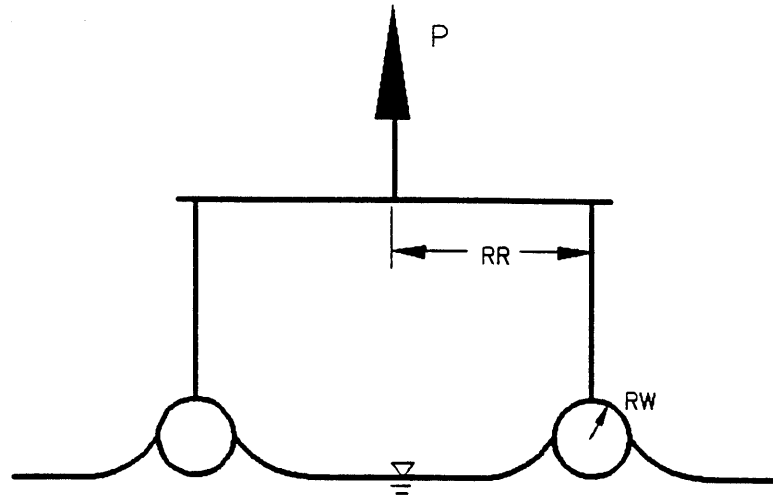
Figure 1: Ring Tensiometer

time interval between successive bubble detachments. As defined, surface time is longer than surface age (Kloubek, 1972a).

2.2.1 Ring Method

The ring method, more formally known as the Lecomte du Nouy ring method (du Nouy; 1918, 1919), is the technique most often used by researchers for static surface tension measurement. The advantage of this method is the complete independence from the necessity of calibration against solutions of known surface tension (Freud and Freud, 1930). Surface tension is defined as the mechanical force necessary to lift a platinum ring of known wire radius (R_W) and ring radius (R_R) from the solution surface (Figure 1). The equation representing this process is:

$$\gamma = \frac{PF}{4\pi R_R} \qquad (4)$$

where:

γ = surface tension;

P = force or pull necessary to detach ring from solution surface;

V = volume of solution displaced by the pull of the ring;

F = Harkins-Jordan correction factor = $f\left(\frac{R_R}{R_W}, \frac{R_R^3}{V}\right)$.

Harkins and Jordan (1930) investigated the theory behind the ring method to develop tables of empirically-determined correction factors for 16 rings with characteristics: $0.4 < R_R < 0.8$ cm, $0.009 < R_W < 0.05$ cm, and 13.9 cm $< R_R/R_W < 78.3$ cm. In addition, they presented possible sources of error associated with ring method:

1. The plane of the ring must be horizontal to the liquid surface. The associated error was proportional to square of the angle of time when the angle was small. This is a necessary condition of the ring method.

2. The diameter of the vessel holding the solution should be greater than 8 cm.

3. The ring should not be warped.

Huh and Mason (1975), presenting a rigorous theory of ring tensiometry, concluded the ring produced excellent results for surface tension measurement using the Harkins-Jordan correction factors. Their correction factors, however, were consistently higher than those of Harkins and Jordan. The authors attributed this difference to their using too small measuring vessels.

Although the du Nouy method was not designed for dynamic surface tension measurement, its application to surfactant solutions has been studied. Lunken-heimer and Wante (1981) investigated the ring method for surface tension measurements and found, like Huh and Mason, that if the diameter of the vessel holding the solution was too small, errors due to straining are appreciable. In addition, they found the maximum pull was dependent on the height between the upper edge of the wetted-wall vessel holding the solution to the solution level for hydrophobic-walled vessels. This indicated the surface layer was connected to a layer of surfactant solution on the wetted-wall. They also observed the velocity of the ring lift affected the measurement of surface tension by increasing the force for faster ring pulls.

The equilibrium surface tension values for surfactant solutions obtained by dynamic surface tension measurements are often compared with surface tension values obtained by static measurements. Caskey and Barlage (1971), Burcik (1950) and Vijayan and Ponter (1972) used the ring method while Thomas and Hall (1975) and Kloubek (1975) used the Wilhelmy Plate as methods to verify the equilibrium surface tension value.

Hommelen (1959) found evaporation, a problem with all liquid surfaces, affected surface tension value. In general, evaporation produced an initial increase in surface tension for surfactant solutions, reached a maximum, then decreased. Decyl alcohol solutions exhibited extreme behavior by experiencing surface tension increases up to 15 hours after the measurement had begun.

Hommelen noted the use of static measurement techniques necessitates the attainment of equilibrium concentration of surfactant solutions. It is difficult to know when equilibrium conditions are reached. As seen from Table 1, time to

10

Surfactant	Time	Reference
Normal nonyl alcohol	10 min.	Hommelen (1959)
Normal decyl alcohol	60 min.	
Capric acid	30 min.	
Dodecyl trimethyl ammonium chloride	< 60 min.	Caskey & Barlage (1971)
Hexadecyltrimethyl ammonium chloride	< 60 min.	
Dodecyl sodium sulfate	< 60 min.	
Hexadecyl sodium sulfate	< 60 min.	
Heptyl & hexyl alcohols	0.01 sec.	Defay & Hommelen (1959b)
Normal octyl branched nonyl alcohols	0.015 sec.	
3,5,5 trimethyl hexanol	0.015 sec.	
0.01 M azelaic acid	>15 hours	
0.5 M adipic acid	0.01 sec.	

Table 1: Time to Reach Equilibrium Surface Tension

reach equilbrium varies by surfactant concentrations and type.

2.2.2 Oscillating Jet Method

The oscillating jet phenomena results from pressurized liquid that is forced through an elliptical orifice which produces a jet with properties of standing waves. The oscillating crests and troughs are the result of surface tension forces in the liquid. Bohr (1909) presented the theory and relationship between surface tension and measurable physical properties such as the flow rate of the liquid, wavelength and major and minor axes radii.

Wavelengths are frequently measured by passing parallel light waves perpendicular to the jet stream. Acting as converging lens, each wave will project a pinpoint of light onto a photographic plate situated at the focal length. As the

surface tension of the liquid jet changes because of surfactant diffusion to the air/liquid interface, each succeeding wave will have longer wavelengths; *i.e.*, will have lower surface tension values. The jet flow rate determines the surface age of each wave.

The main advantage of the oscillating jet method is the accuracy with which the surface age can be determined. Whereas the surface age from drop techniques are often unknown because of the failure to recognize the moment of surface formation, surface age in the oscillating jet begins at the moment of departure from the orifice. Exact flow measurements yield an excellent estimate of the velocity of the jet. The velocity at the center and the velocity at the edge of the stream; however, are not the same. Most researchers neglect this small difference although Jobert and Leblond (1979) argue for the inclusion of surface velocity profiles along the jet. They state the oscillating jet method is unsuitable for determining the dynamic surface tension of surfactant solutions if the surface velocity profile is not included in the calculations.

Another advantage of the oscillating jet method is surface tension at surface ages from as early as 0.001 sec have been recorded. This ability to calculate surface tension at such early ages is probably the key to resolving the question of the existence of dynamic surface tension for pure liquids. Pure water exhibited dynamic surface tension values for surface ages less than 0.005 sec after which the values remained constant (Thomas and Potter, 1975). Caskey and Barlage (1970), also using the oscillating jet, claimed the surface tension values of pure water remained unchanged with time for the surface ages of 0.004 to 0.24 sec — the range of their investigation. Clearly the range of surface ages determined the answer to the question.

The effect of the orifice configuration and orientation have some significance on the resulting values of surface tension. Thomas and Potter (1975) working on both aspects, concluded the extension of the Bohr equation for vertically oriented jets was not valid for horizontal jets. They also developed a relative method for determining the dynamic surface tension values of liquids based on measured values of water determined from the same orifice and orifice orientation. This eliminated the dependence on capillary orifices. Defay and Hommelen (1958) also addressed the problem of orifice dependence and defined a criterion whereby careful orifice selection eliminated the dependence. In the quest for capillary orifices which met their criterion, of the 50 capillaries made, only seven were acceptable.

In addition to the disadvantages of orifice selection and dependence, the cost of equipment can be prohibitive to the selection of this method. The nature of the parameters necessitates measurement with sophisticated equipment because of the high degree of accuracy required in measuring wavelengths and jet radii. This accuracy translates to high equipment costs.

2.2.3 Drop Methods

The basic premise of drop methods is surface tension can be calculated from the physical characteristics of the drop as it forms at the end of a capillary tip of known external radius. The generic label of "drop methods" encompasses techniques identified by the physical quantity measured: pendant drop (shape), drop-weight, and drop-volume. Although these methods are interrelated, the drop-volume is preferred because of ease in measuring.

The pendant drop method relies on the hanging drop shape to determine the parameter values necessary to compute surface tension. Pierson and Whitaker

13

(1974) investigated the shape of the pendant drop to find the drop volume was always less than the pendant drop volume. The stability of the hanging drop was found to be dependent only on its shape.

The only difference between the drop-weight and drop-volume methods lies in the selection of the volume or weight measurement. The drop-weight has been extensively used because of the speed and accuracy in which measurements can be made. However, with the increased accuracy in microburets, it has become equally advantageous to use the drop-volume technique.

A major problem of drop methods is the determination of surface age. The surface age is generally taken to be the time interval from drop formation to drop detachment. Surface tension lowering due to surfactant diffusion to the surface results in drop detachment. Surface age is a function of the measuring technique of the experimenter who must subjectively define the start of the surface. In addition, Hommelen (1959) found subsequently formed drops were contaminated with drop residue from previous drops and that drops with long surface ages were subject to evaporation effects.

2.2.4 Maximum Bubble Pressure Method

The maximum bubble pressure method is based on the maximum presssure in a capillary or a maximum pressure difference between two capillaries of different radii necessary to produce and detach a bubble from a capillary tip immersed in a test solution.

One of the first maximum bubble pressure measuring apparatus for surface tension is attributed to Sugden (1922). Two capillaries of different radii were sealed onto a test tube containing the test liquid by a rubber stopper. The capillaries,

14

open to the atmosphere, could be opened and closed to air flow by rubber stoppers. By releasing mercury from a flask into a beaker a pressure drop was created in the system and air was pushed into the capillary to form a bubble. Capillary radius and mercury flow rate controlled the bubble formation rate.

Bendure (1971) used argon gas to create pressure in the system to form bubbles at a capillary tip. The bubble pressure was sensed by a Bourdon tube pressure gauge capable of pressure differentials of 300 torr. A resistor converted the current output to voltage which was recorded on a strip chart.

Again, the major difference between dynamic and static surface tension measurements is a careful accounting of surface age. In the maximum bubble pressure measuring technique, the time interval between bubble detachments (surface time) is usually defined as a composition of surface age and dead time.

surface age is the time interval from the start of the fall of the meniscus to the start of the formation of the bubble at the top of the capillary.

dead time is the time interval from the end of the surface age to bubble detachment (period of rapid bubble growth).

Most of the adsorption process of surfactants to the interface occurs during the surface age. In this period, the surface area remains constant so the calculation of adsorption is fairly easy. During dead time, the rapid bubble growth prohibits adsorption of surfactant on the surface. It is apparant at low bubbling frequencies dead time is not as important as during high bubbling frequencies when dead time can be a significant part of surface time. Austin, *et al.* (1967) gave dead time corrections of $31.9 - 0.000425S$ msec where S is the bubbling frequency. This empirically-determined correction factor is independent of capillary radius

15

for capillaries with heads between 19.7 to 26.4 cm of pure water at the maximum bubbling frequency. The authors believe 10 msec to be the shortest surface time before errors occur.

Kloubek (1972a,b) did extensive work in the maximum bubble pressure methods. His results include:

1. The volume of the bubble is independent of the capillary tip immersion depth.

2. The diameter of the detached bubble increases linearly with capillary diameter.

3. Capillary orientation affects the bubble separation process.

4. A decrease in bubble volume is experienced with an increase in bubble frequency.

5. There exists a maximum bubbling frequency at which only dead time exists and above which pressure is no longer related to surface tension.

2.2.5 Summary

This section reviewed the popular surface tension measuring techniques to identify the one most suitable for this project. Clearly the ring method is unsuitable for dynamic surface tension measurements but it gives an excellent equilibrium surface tension value. The drop methods rely on capillary tip shapes which can lead to large error and surface age is difficult to identify. The oscillating jet has the advantage of giving the earliest surface age and is very accurate but requires the most expensive equipment set-up costs of any method and cannot be used for

long adsorption times (> 2 sec). The maximum bubble pressure method is the method of choice for its accuracy, the early surface ages and the low equipment costs.

Table 2 summarizes the results of various researchers in the dynamic surface tension field.

2.3 Surfactants

The body of work addressing the types of surfactants and their effect on aqueous solutions is voluminous. The next section gives a general overview of surfactants and their effect on mass transfer. The following section discusses a specific aspect of surfactants in aqueous solutions – foaming.

2.3.1 Surfactants and Mass Transfer

The following are a few generalizations regarding surface tension and surfactants, followed by a discussion of surfactants and dynamic surface tension.

1. High concentrations of surfactants lower surface tension relative to the pure solvent state. The surfactant concentration that produces a maximum surface tension decrease and above which additional surfactant has no effect on surface tension, is called the critical micelle concentration (CMC) (Caskey and Barlage, 1971). Furthermore, the steeper decrease in surface tension is evident only at high surfactant concentrations.

2. Using the Wilhelmy plate method, Lange (1965) found suface tension is dependent on its prehistory. Compressing the surface once or twice alters

17

Table 2: Dynamic Surface Tension Measurements

Description	Comments	References

Drop Methods

Drop-length, drop-volume and drop-weight methods rely on accurate drop characteristics measurements to determine surface tension. The main disadvantages of these methods are difficulty in determining short surface ages and accounting for the effect of the expanding surface.

Description	Comments	References
Drop-length	Difficult to establish surface ages.	Hommelen (1959)
Drop-volume	Pulses generated by an oscillator control drop volume. Used Harkins & Browns correction factors.	Tornberg (1977)
	Ward-Tordai equation was not valid for changing surface area. Assumed spherical shape of the drop	Joos, et al. (1981)
Drop-weight	Used one stalagmometer. Corrections of Harkins & Brown were applicable only when drop formation time was long. Each point represented a separate test so the results were reproducible.	Kloubek (1975)
	Used various stalagometers.;Kloubek, et al. (1976) $0 \leq t \leq 100$ sec	
	Drop shape and stability were discussed for $t < 20$ sec.	Pierson, et al. (1976)
	Rate at which drop break-up occurred was dependent directly on surface tension, and capillary radius but inversely proportional to fluid density and the square of the viscosity.	

Dynamic Surface Tension Measurements (Continued)

Description	Comments	References

Oscillating Jet Method

Test solution is forced through an elliptical orifice producing a stream with oscillating wave characteristics. The wavelength and radii (maximum and minimum) of each wave determines surface tension while wave position determines surface age. The main advantage in this method lies in the accuracy in which the surface age can be calculated.

Description	Comments	References
Light beams were used to find wave characteristics. Radii measured by calibrated moving rectilinear eyepiece.	Eliminated dependence of capillary orifice on surface tension values by standardizing with solutions of known surface tension and application of correction factors.	Defay, et al. (1958)
Two-coordinate cathetometer was used to measure wave characteristics from a photograph. Orifice was constructed of Mylar film attached to stainless steel tubing nut. Vertical jet orientation.	Water may have dynamic surface tension for $t < 0.006$ sec.	Caskey, et al. (1971)
Parallel light beams were used to define waves. Wave characteristics were measured off of photographic negatives by a measuring comparator.	At low surface ages, surface tension was dependent on liquid flow rate. At higher ages it became independent of flow rate. Water exhibited dynamic surface tension behavior. Bohr's equation was applicable for ages $t > 0.006$ sec.	Vijayan, et al. (1972)
Uniform and bell-shaped glass capillary orifices were used. Vertical and horizontal orientations were used.	Surface tension depended on orifice orientation. Evidence of dynamic surface tension for distilled water for $t > 0.006$ sec. Relative method of determining true surface tension values was proven to be valid.	Thomas, et al. (1975)

19

Description	Comments	References

Maximum Bubble Pressure Method

This method is based on the maximum pressure needed to liberate bubbles from a capillary submerged in test solution. Pressure increases are measured as functions of time.

Description	Comments	References
One capillary, stroboscope was used to measure bubble frequencies. Filming techniques were used to determine surface age.	Determined that the limit to maximum bubbling frequency occurred when time of bubble formation approach dead time. $0.010 \leq t \leq 0.120$ sec.	Austin, et al. (1967)
One capillary, used water passing through a rotameter to measure air flow rate.	Most adsorption occurred when surface area was constant. Diffusion-controlled mechanism of mass transfer $t < 100$ sec.	Bendure (1971)
Two capillaries, stroboscope was used to measure bubble frequency.	Volume of the bubble was independent of capillary tip immersion depth. Diameter of the detached bubble increased linearly with increasing capillary diameter. Existence of maximum obtainable bubbling frequency confirmed.	Kloubek (1972)

20

the equilibrium value of surface tension.

3. Surface tension decreases with increasing temperatures (Tornberg, 1977). This decrease can be attributed to the higher surface activity at the higher bulk temperatures. At equilibrium, surface tension increased with temperature or remained constant (Kloubek, 1972b).

Contaminates on the gas/liquid interface can affect the dynamic surface tension measurement. In drop stability analysis, for experimental times less than 200 sec, surface tension appeared to be constant for an 0.08M hexanoic acid (Pierson and Whitaker, 1976). After 200 sec, surface tension increased with time. Slow adsorption of contaminates in the system was postulated for this anomaly. Gilanyi, *et al.* (1976) attributed the competitive adsorption process of contaminates as the mechanism for prolonged time dependence of surface tension which could not be explained solely by diffusion. They supported the theory that a necessary condition for surface purity is an absence of a minima in the γ versus ln C curve. Surface purity depends on surface life time and experimental method.

The effect of electrolytes has been studied by a few researchers. Lauwers and Ruyssen (1964) found the addition of electrolytes (sodium salts: NaCl, Na_2SO_4, Na_2HPO_4 and NaH_2PO_4) decreased surface tension in solutions of β-lactoglobulin. Solutions of Maxonol (0.0003M to 0.003M) exhibited sharp increases in the initial rate of surface tension decrease in 0.027M NaCl solution (Austin, *et al.*, 1967). The effect of NaCl on surfactant solutions was also dependent on the type of surfactant (Shah, *et al.*, 1978). Nonionic surfactants seemed to exhibit no change in surface properties. Burcik (1950) attributed the decrease in surface tension could be attributed to the charge accumulation in the diffusive layer repelling

21

the approaching surfactant molecules, assuming the surfactants were ionic. This was supported by an experiment in which nonionic surfactants did not exhibit electrolyte effects in surface tension measurements.

Surfactant orientation may also influence dynamic surface tension measurements. When the oscillating jet was used as the measurement technique, a common feature of surfactant solutions appeared to be the contraction of wavelengths for very early surface ages and an extension of wavelength for longer surface ages. For early ages, the surfactant was not allowed the opportunity to orient the hydrophobic group to be outside the jet. At longer ages the polar orientation becomes established so the hydrophobic group lies outside of the surface, allowing for the surface tension decrease (Thomas and Hall, 1975).

The mechanism of mass transport is of great interest in surfactant study. There is a general concensus the diffusion process describes the mass transport of surfactants to the air/liquid interface. However, controversy arises over the existence of an energy barrier at the surface.

Proponents for the existence of the barrier see it as a subsurface layer between the bulk solution of the surface. The surfactant molecules are instantaneously in thermodynamic equilibrium at the bulk/subsurface interface (a Ward-Tordai assumption). The concentration gradient from the bulk to the surface promotes the diffusion of surfactants to the surface, during which time surface concentration can be related to time by:

$$\Gamma = 2C_\circ \left(\frac{Dt}{\pi}\right)^{1/2} \tag{5}$$

where:

Γ = surface concentration;

D = diffusivity;

C_o = bulk concentration;

t = time.

This equation does not allow for desorption. As the finite active sites of the surface become occupied, back diffusion occurs from the surface to the bulk. At this time, the full Ward-Tordai equation (which relates surface concentration to time and includes desportion) governs. Defay and Hommelen (1959) found the low values of calculated γ supported the existence of the barrier.

Suzuki, *et al.* (1972) observed for bubbles in air, surface tension increased with time, reached a maximum, then decreased. In the rising portion, they speculated the depth of the surface layer decreased with time as the bubble increased in surface area, therefore, the surface tension increased. In the latter region, the subsurface layer became the surface layer, therefore, surface tension decreased by increased mass transport of surfactants to the surface.

Contrasting the above, Lange (1965), using the Ward-Tordai and the v. Szyskowski equations, concluded time dependence of surface tension was controlled by diffusion through a diffusive layer whose thickness increased with time. This diffusive layer, therefore, was unaffected by convection from the bulk solution.

Of those opposing the existence of the barrier, Joos and Rillaerts (1981) suggested the Ward-Tordai equation was not applicable to the expanding surface of the bubble methods, and that convection near the surface occured due to the motion of the expanding surface. For short adsorption times, the equation describing

the surface concentration with convection was given by:

$$\Gamma = 2C_o \left(\frac{3Dt}{7\pi}\right)^{1/2} \tag{6}$$

A dilation time was included for the expanding surface yielding:

$$\Gamma = 2C_o \left(\frac{Dt}{\pi(2\alpha + 1)}\right)^{1/2} \qquad \theta = \frac{\alpha}{t} \qquad 0 \leq \alpha \leq 2/3$$

when $\alpha = 0$ this equation reduced to the first term of the Ward-Tordai equation. Deviation from the spherical shape occurred when $\alpha > 2/3$. This equation was tested on Bendure's (1977) data and they concluded no barrier from diffusion need be postulated.

Bendure (1977) derived equations for short-term and long-term adsorption times based on a Langmuir description of adsorption processes. The equations relating dynamic surface tension to time were:

$$\gamma - \gamma_\infty = \frac{\Gamma^2 RT}{(\pi D)^{1/2} C_o t^{1/2}} \qquad \text{long adsorption time}$$

$$\gamma - \gamma_o = C_o 2RT \left(\frac{D}{\pi}\right)^{1/2} t^{1/2} \qquad \text{short adsorption time}$$

where:

R = universal gas constant;

γ_∞ = equilibrium surface tension;

γ_o = surface tension of pure solvent.

For long adsorption times, the above equation shows $\gamma - \gamma_\infty$ versus $\frac{1}{\sqrt{t}}$, and for short adsorption times, $\frac{\gamma - \gamma_o}{C_o}$ versus $\sqrt{t}$, should be linear. Using estimates of the diffusivity constant found from the limiting cases of both adsorption times, the data using four surfactants (dimethyl decylphosphine oxide, dimethyl dodecylamine oxide, dimethyl dodecylphosphine oxide and n-dodecyl hexaoxethylene glycol monoether) at various concentrations were plotted using both equations. The plots

24

confirmed the "correctness" of the equations and assumptions.

Kloubek (1972b) proposed another manner to test the equilibrium surface tension of surfactant solutions. A plot of $\frac{1}{\gamma_\infty - \gamma}$ versus $\frac{1}{\sqrt{t}}$ was used in the maximum bubble pressure method with sodium dodecyl sulfate. As $\sqrt{t} \to 0$, equilibrium surface tension should be reached. At low concentrations of surfactant (0.00076M and 0.00088M) the relationships were nonlinear; at higher concentrations the relationships were approximately linear in the surface age range t < 10 sec. Extrapolation of the curves by extension of the linear portion of the curves gave better results than the extension of the fitted curve. Kloubek (1975) also used $\frac{1}{\gamma_\circ - \gamma}$ versus $\frac{1}{t}$ to determine the equilibrium surface tension for results by the drop method. In this case, although the range of values was great, the average value agreed well with the static method determination.

2.3.2 Foaming

Foaming is an important aspect of surfactant characteristics since foaming can be a nuisance in aeration basins and is related to surface tension. This section will only address foam production by gas injection into a liquid phase.

Foam is composed of gas pockets surrounded by thin films; therefore, a study of film properties is necessary before foam can be discussed. The film between bubbles which compose the foam are called the lamella of the foam. The equation relating the pressure change (Δ P) across these lamellae is described by the Young-Laplace equation:

$$\Delta P = \gamma(\frac{1}{R_1} + \frac{1}{R_2})$$

R_1 and R_2 are the radii of curvature at a point on the lamella. R_1 and R_2 swing in

perpendicular planes to the surface and to each other. This equation determines the shape of the films formed on wires dipped in surfactant solutions (Bikerman, 1973).

Pure solutions do not foam because gas bubbles beneath the liquid surface rupture upon contact with each other or with the surface since no surfactants are available to adsorb to the surface to decrease the surface tension. Lamellae cannot be formed by inelastic surfaces. Film elasticity is a necessary but not sufficient condition for foaming (Bikerman, 1973).

The effect of gravity on the lamella is to drain the liquid from the film such that the top of the film becomes thinner with the bottom becoming thicker. It is not the overall thinning that results in film rupture but a localized thinning at a particular spot. At a local thin spot, the surface tension is slightly higher than the immediate surrounding area because the concentration of surfactants in that spot is lower. Mechanical film response to thin spots is known as the Marangoni-Gibbs effect. The Gibbs effect is a change of surface tension with a change in the surface-active solute concentration based on an equilibrium value of surface tension. The Marangoni effect is a change in surface tension with time and is based on an instantaneous surface tension value. These effects are complimentary, both describe the same effect. A surface tension gradient exists at the thin spot resulting in the movement of liquid from surrounding areas to that spot leading to the physical restoration of the film. The liquid from the surrounding areas also brings surfactant molecules to the spot to reduce surface tension and the spot regains local equilibrium with the surrounding areas. If the draining occurs at a faster rate than the restoring Marangoni-Gibbs effect, the film ruptures (Rosen, 1978).

Foams are composed bubbles. When three or more bubbles meet, the intersection point of all lamellae is called the Plateau border (Bikerman, 1973). Bubbles assume positions as dictated by capillary pressure and surface tension. For three bubbles, the angle formed by the lamellae is 120°; each lamella pulls at the Plateau border by force/unit length of 2γ. These equal forces acting on a point, balance only if the angles between them are equal, *i.e.*, 120°. The most stable foam structure occurs when three bubbles meet at the Plateau border.

Foam stability has been discussed by several researchers (Jones, *et al.*, 1957). There is, however, no consensus on the definition of foam stability uniformly adopted by all in the field, although the Ross-Miles test is the most frequently used. Presented below are various tests of foam stability.

1. Pour foam test (also known as the Ross-Miles test). 100 ml of solution is allowed to fall through a height of 70 cm from a separatory funnel into a graduated cylinder. Both the time until total initial foam breakdown and time to break initial foam volume to one-half are taken as measures of foam stability (Burcik, 1950).

2. Single bubble test. The average lifetime of 20 to 30 uniformly sized small bubbles in CO-free water was taken as a measure of foam stability (Burcik, 1950).

3. The minimum volume of solution drained from the foam after a specified length of time (Shah, *et al.*, 1978).

4. Foam stability was defined as $\theta = \frac{G}{d}$, where G = total volume of the dispersed gas obtained when foam volume (V) and liquid content (L), reached a maximum, G = V - L. (d = calibrated gas flow rate). θ was dependent

only on the physiochemical properties of the solution (Lauwers and Ruyssen, 1964).

5. The ratio of the initial height of the foam column, H_o, from the Ross-Miles foam test to the height of the foam column after 5 minutes, H_5. K = foam stability = $(H_5/H_o)100$ (Chistyakov, *et al.*, 1979).

Some factors affecting foam stability are:

1. In a steric acid — steryl alcohol solution, tight packing of surfactant molecules at the interface was correlated with maximum foam stability (Shah, *et al.*, 1978).

2. Solutions of triethanolamine (TEA) salts of alkyl phosphates and TEA salts of individual mono- and didodecyl phosphates showed foam stability increased as surfactant concentration increased (Chistyakov, *et al.*, 1979).

3. Protein solutions of β-lactoglobulin showed a sharp decrease in foam stability at a pH associated with the isoelectric point of the protein (Lauwers and Ruyssen, 1964).

4. Low gas flow rates produce more stable foam because of the more regular bubble shapes rather than bubble coalescence (Joos and Ruyssen, 1964).

5. High foam stability favors (1) low surface tension in relation to that of the pure solvent, (2) moderate rate of surface tension lowering, and (3) high bulk or surface viscosity (Burcik, 1950).

Antifoam agents or foam inhibitors act to suppress foam production or destroy existing foam through increased foam drainage and surface tension increases.

28

There is no correlation between properties of an antifoam agent and properties of the foamy solution. Many foam suppressors can work on a particular solution (Bikerman, 1973).

2.3.3 Summary

The effect of surfactants on dynamic surface tension measurements, the adsorption mechanism and foaming were discussed in this section. Table 3 presents some data of surfactants and dynamic surface tension measurements.

2.4 Oxygen Transfer Review

Oxygen transfer from the bubble to a liquid occurs in three phases:

1. transfer from the interior of the bubble to the interface;

2. transfer through the interface by molecular diffusion and;

3. transported away from the interface by diffusion and convection (Mancy and Okun, 1965).

The rate of oxygen transfer is controlled by molecular diffusion under laminar conditions or surface renewal rate under turbulent conditions (Eckenfelder and Ford, 1968).

Pasveer (1955) was able to determine the "time of contact" of a stagnant film for bubbles 1–3 mm in diameter. He concluded the bubble travels through the water without turbulence. The conceptual mechanism describing transfer is

Table 3: Surface Tension Measurements of Surfactant Solutions

Surfactant	Method	Concentrations	Time Interval	Comments	Reference
Sodium dodecyl sulfate	Drop-weight	3.3, 5.9, 8.1 } $\times 10^{-3}$ M (25°C)	$0 \leq t \leq 150$ sec	At higher concentrations, lower surface tension values were exhibited for the same surface age.	Kloubek (1975)
		1.7×10^{-3} M (25°C)	$t < 0.2$ sec	Surface tension versus bubble intervals (t) and surface age (T).	
	Maximum bubble pressure	3.3 (25°C), 3.3 (20°C), 1.7 (25°C), 1.7 (22°C), 1.7 (20 C) } $\times 10^{-3}$ M	$t < 1.0$ sec.	Increase in temperature corresponded to higher surface tension values for the same surface ages.	Kloubek (1972)
		0.76, 0.88, 1.70, 3.3, 5.9, 8.1 } $\times 10^{-3}$ M (25°C)	$T < 0.3$ sec.	Lower concentrations exhibited higher surface tension values for the same surface age.	
		3.3 (20°C), 3.3 (25°C), 5.9 (25°C), 8.1 (25°C) } $\times 10^{-3}$ M	$T \cdot 0.015$ sec		
	Oscillating jet	5.0×10^{-3} M	$t < 0.08$ sec		Thomas, et al. (1975)
		4.0×10^{-3} M		Recrystallized and foam fractionated solutions.	Gilanyi, et al. (1976)
		4.1×10^{-3} M		Recrystallized.	
Hexadecyl sulfate	Drop-weight	6.1×10^{-6} M	$t < 600$ sec.	Effects of contaminates on recrystallized SDS solutions.	Gilanyi, et al. (1976)
Lauryl alcohol		3.1×10^{-6} M			

Surfactant	Method	Concentrations	Time Interval	Comments	Reference
Dodecylamine Hydro-chloride	Maximum bubble pressure	5×10^{-3} M			Kloubek (1972)
Carbowax 6000		0.025 0.075 0.10 0.25 } $g/_{cm}3$	t < 0.060 sec	Low concentrations exhibited higher surface tension values for the same surface ages. Higher concentrations had greater changes of surface tension with time. Noticible was a local maximum surface tension value after an initial decline.	
Carbowax 1540	Oscilliat-ing jet	0.005 0.01 0.025 0.10 } $g/_{cm}3$	t < 0.060 sec		
Sodium Di-(2-ethyhexyl) sulphosuccinate		0.075 0.0875 0.10 } $g/_{cm}3$	t < 0.060 sec		Thomas, et al. (1975)
Teepol L		0.25 0.50 0.10 5.0 } g/cm^3	t < 0.060 sec		
Cetyltrimethylammonium bromide		0.025 0.050 0.10 0.18 } g/cm^3	t < 0.060 sec		

31

Surfactant	Method	Concentrations	Time Interval	Comments	Reference
Sodium di-(2-ethylexyl) sulphosuccinate	Oscillating jet	$0.05g/100cm^3$	$0 \leq t \leq 0.070$ sec		Thomas, et al. (1976)
Heptanoic Acid	Drop weight	$1.5 \times 10^{-2} M$	$1 \leq t \leq 1000$ sec	Definite minimum surface tension value exhibited after which surface tension increased.	Pierson, et al. (1976)
Hexanoic Acid		$8 \times 10^{-2} M$	$1 \leq t \leq 1000$ sec		
Dimethyl-decylphosphine oxide ($DC_{10}PO$)		0.00063% 0.0024% 0.0068% 0.014% 0.048% 0.137%		Various stalagmometers were used. Shows $\dfrac{\gamma_o - \gamma}{C_o} \times 10^3$ vs. $\sqrt{t}$ γ_o = initial surface tension (not necessarily @ t = 0) γ = surface tension @ time t C_o = initial surfactant concentration	
Dimethyl-dodecyl phosphine oxide ($DC_{12}PO$)	Maximum bubble pressure	0.00066% 0.0015% 0.0030% 0.0060%	$10 \leq t \leq 100$ sec	Plots revealed straight lines for each surfactant at all experimental concentrations. A diffusion model was presented.	Bendure (1971)
Dimethyl-dodecylamine oxide ($DC_{12}AO$)		0.001% 0.0021% 0.0039% 0.0064% 0.013% 0.020% 0.056%			
N-dodecylhexaoxy-ethylene glycol monoether ($C_{12}E_6$)		0.00058% 0.00083% 0.0024% 0.0034% 0.0076%			

the interfacial film rests at the surface and is instantaneously replaced by a new interfacial film after a set period of time. Pasveer confirmed the penetration theory for oxygen transfer. However, his experiments were done at low flow rates of 20–80 ml/min which are never used in wastewater practice. Using higher air flow rates, it is expected the surface renewal theory would dominate.

The transfer of oxygen is also a function of the bubble life in the aeration tank which can be described by three phases:

1. Bubble formation. During bubble formation the interfacial area continually expands, creating new surface area; at this moment the large concentration gradient promotes rapid mass transfer. In addition, the gas inside the bubble is generally in turbulent motion, creating high shear stress, thus also promoting gas transfer.

2. Bubble rise. In diffused aeration, bubbles rise at terminal rise velocity. The transport of oxygen during this phase is assumed to be steady state. Bubbles have highly elastic surfaces which responds to mechanical shocks (Mancy and Okun, 1960).

3. Bubble burst. As bubbles break at the top of the aeration basin the oxygen enriched interfacial film of the bubble deposits over the surface of the basin increasing bulk oxygen concentration. The turbulent nature of the surface also enhances atmospheric reaeration.

The overall liquid film coefficient, K_L, can similarly be divided to represent transfer in the three phases of bubble formation ($K_L(f)$), bubble rise ($K_L(r)$) and bubble burst ($K_L(b)$), *i.e.* ,

$K_L(f)$ A rigorous formulation of oxygen transfer quantities during bubble formation has not been achieved. It is estimated 20–25% of the total transfer occurs during bubble formation (Barnhart, 1969). $K_L(f)$ also appears to be a function of diffuser type. Small quantities of oxygen are transferred during bubble formation for spargers as compared to transfer using Saran tubes. For diffused aeration, oxygen transfer during bubble formation can be an appreciable fraction of total oxygen adsorption. Bubble formation resulting from bubble break-up during rise involves some oxygen transfer, but the effect is thought to be negligible (Bewtra and Nicholas, 1964). Oxygen transfer during the formation time is thought to be the highest for a column (Pasveer, 1955).

$K_L(r)$ The transfer coefficient during bubble rise is assumed to be a constant, since rise velocity and bubble shape remain unchanged.

$K_L(b)$ Data on the oxygen transfer coefficient due to bubble burst at the surface is also scarce. Oxygen transfer due to surface aeration itself can be appreciable, but the contribution by the oxygen saturated layer of the bubble is thought to be negligible (Bewtra and Nicholas, 1964).

Complicating the conceptualization of oxygen transfer is the expansion of the bubble as it rises and the simultaneous shrinking as oxygen is depleted. Ippen and Carver (1954) found the volume correction for expansion of air bubbles was unnecessary as its effect on oxygen transfer was negligible. Absorption of oxygen is highest when the dissolved oxygen concentration in the tank is low (the concentration gradient is highest). However for air bubbles, the loss in size due to oxygen depletion is sometimes more than compensated by the increases resulting

from expansion. They also noted the rising bubbles set downward currents in motion carrying the highly saturated surface water toward the bottom, resulting in a more evenly distributed oxygen concentration throughout the tank.

Barnhart (1969) showed oxygen transfer was highest at a bubble radius (R_b) of 1.1 mm. When $R_b < 2.0$ mm, gradual increases in oxygen transfer occurred. $1.1 < R_b < 2.0$ mm small changes in bubble sizes influenced the oxygen transfer rate with smaller bubbles being more efficient. When $R_b < 1.1$ mm the transfer quantity decreased significantly although the surface area was large, indicating a change in the nature of the film.

2.4.1 Surfactant Effects on Oxygen Transfer

The surfactants adsorb at the gas/liquid interface in a constructed, usually charged, monolayer. At the CMC, the adsorbed film is most compact (highest surfactant concentration per unit of interfacial area) and the monolayer has the maximum thickness. If surfactants are added past the CMC, a multilayer of molecules adsorb at the interface (Mancy and Okun, 1960). Surfactants tend to: (1) stabilize the interface, making the gas/liquid interface more rigid (Lister and Boon, 1973), (2) decrease renewal (Eckenfelder, *et al.*, 1956), and (3) increase interfacial viscosity (Yoshida and Akita, 1965; Mancy and Okun, 1960).

The stabilization of the interface makes normally fluid particles behave as rigid bodies. Haberman and Morton (1953) found when $0.3 < R_b < 3.0$ mm, the terminal rise velocities of air bubbles in filtered water were higher than those bubbles in tap water. This difference was attributed to the adsorption of minute particles imparting rigidity to the interface in the tap water system. Similarly the rigid interface decreases the internal circulation of the gas in the bubble (Motarjemi

and Jameson, 1978) and increased surface drag because of higher surface viscosities tend to decrease terminal rise velocities. The decrease in terminal rise velocity implies longer bubble retention times in the aeration basin, therefore increases in oxygen transfer might be expected.

Mancy and Okun (1960) noted as the concentration of surface active agents (SAA) at the interface increased, the time of bubble formation and bubble volume decreased. Both reactions can be explained by lower surface tension values in the presence of SAA decreases the elasticity of the interface; therefore, shear forces create bubbles at a faster rate and smaller in size. The smaller bubbles also have greater retention times and more total surface area. However, the adsorption of the surfactants onto the gas/liquid interface decreases K_L. Surfactants at the interface decrease the available surface area for molecular diffusion, and form a hydration layer at the surface, resulting in higher surface viscosity and increased thickness of the surface layer, thus increasing the resistance to oxygen transfer. Both mechanisms support the premise of the decrease in oxygen transfer in the presence of surfactants (Mancy and Okun, 1965). However Carver (1956) observed a decrease in K_L in surfactant solutions even though the reduction in shear forces at the boundary layer resulted in decreased terminal rise velocity, reduced oscillatory motion and increased drag.

Furthermore, surface tension gradients on bubbles affect bubble shape, thus affecting terminal rise velocities. Surface tension gradients develop on the surface of the rising bubble such that higher surface tension values are located on the top of the bubble. This gradient results from surface renewal and promotes the formation of a rigid cap. The terminal rise velocity corresponded to an equilibrium cap size. For a given surfactant, the completely rigid sphere can be associated with a given

bubble size. The time to reach terminal velocity increases with bubble size and with low surfactant concentration (Detwiler, 1979). Barnhart (1969) correlated bubble shape with Reynold's number and found:

Re < 300   Spherical bubbles act as rigid spheres.

                The rise is characterized as rectilinear or helical.

300 < Re < 4000 Bubbles have ellipsoidal shape.

                The rise is characterized as rectilinear, rocking motion.

Re > 4000   Bubbles formed spherical caps.

Mancy and Okun (1965) attempted to qualify the decrease in oxygen transfer in the presence of surfactants by describing the resistance to transfer in two parts.

1. Surfactants do not physically add any resistance to mass transfer but tend to inhibit hydrodynamic activity of the gas/liquid interface.

2. The interfacial film of surfactant molecules forms a viscous hydration layer and decreases the number of sites available for oxygen molecules to diffuse to the surface.

Their experiments using Aerosol OT in stirred aeration beakers identified the region of resistance to mass transfer.

$$Re \leq 4.6 \times 10^3 \qquad \text{Region I — Laminar}$$
$$4.6 \times 10^3 \leq Re \leq 6.7 \times 10^3 \quad \text{Region II — Transition}$$
$$Re \geq 6.7 \times 10^3 \qquad \text{Region III — Turbulent}$$

In Region I total resistance decreased with increasing Re which suggested surfactants had no effect on resistance. The bulk resistance (transfer through the bulk solution by diffusion and convection) was very high, masking the changes in

37

surface resistance caused by surfactants. In Region III, oxygen transfer was dependent on surface renewal, again no apparent effect of SAA could be identified. But in Region II, surfactant effects could be identified. It was concluded the main resistance to transfer comes from the formation of the viscous hydration layer and decrease in the number of transfer sites.

Mancy and Barlage (1968) extended Mancy and Okun's (1960, 1965) work and concluded surfactants are effective at reducing gas transfer rates but the reduction is dependent on the aeration technique. Furthermore, mass transfer reduction, whether due to a physical barrier inhibiting diffusion through the interface or to formation of the hydration layer, is largely a function of the structure and physiochemical characteristics of the surfactant molecule as well as aeration technique.

Two opposing mechanisms affect the overall transfer of oxygen in aeration. The increase in surface area promotes transfer, whereas the decrease in K_L inhibits transfer. Mancy and Okun (1960) indicate higher $K_L a$ values are obtained in the presence of surfactants. They showed K_L decreased sharply with increasing surfactant concentration until the CMC, afterwhich K_L remained unchanged with further surfactant concentration increases. However, $K_L a$ continued to increase with increasing surfactant concentration indicating the total surface area over-compensates for the loss in K_L. Others contend the increase in surface area does not offset the decrease in K_L (Lister and Boon, 1973; Otoski, et al., 1978; Eckenfelder, et al., 1956).

Eckenfelder and Ford (1968) also show the degree of mixing plays a role in determining oxygen transfer. Under laminar conditions the stagnant film theory dominates; therefore, the α value is unaffected because the interfacial resistance to transfer is less than the resistance in the bulk solution. As turbulence increases,

38

α decreases because the interfacial resistance governs the transfer rate. At highly turbulent conditions, α increases since the surfactants cannot establish an interfacial film for mass transfer resistance, the surface renewal rate is high.

Characteristics of surfactants on oxygen transfer have been investigated by Lynch and Sawyer (1960). A summary of their findings include:

1. The higher number of carbon atoms (n) in the alkyl group of surfactants polypropylene benzene sulfonate, straight-chain alkyl benzene sulfonates with attachment at the second carbon atom and normal straight-chain alkyl benzene sulfonates, decreased the gross oxygen transfer coefficient for the same concentration of surfactants in different synthetic waters. The normal straight-chain alkyl benzenes sulfonates showed an increase in the volumetric oxygen transfer coefficient starting from n = 10 - 12 in synthetic waters of known hardness. This reversal in trend was attributed to insolubility of the surfactant in the solution.

2. The length of the hydrophilic ethylene-oxide group in nonionic fatty esters affected oxygen transfer. The large ethyloxyl group corresponded to lower oxygen transfer coefficient. For nonionic fatty amides, longer ethoxy group corresponded to higher value of $K_L a$.

3. Ionic nature and chemical configuration of the hydrophilic group was important.

A consequence of surface tension reduction with surfactants, especially in aerated wastewater treatment systems, is the production of foam. Although foam often requires no additional treatment expenses it has an unsightly appearance,

it is difficult to clean dried foam residue, and it can be messy (Metcalf and Eddy 1979). Little research has been conducted on foaming effects or antifoam agent effects on oxygen transfer.

Lynch and Sawyer (1954) used a narrow column (4 inch I.D., 9 ft long) to investigate the foaming capability of 11 commercial detergents. They found no correlation between the type of surfactant (anionic or ionic) and foam production (or non-production). They noted frothing is temperature dependent with warmer temperatures promoting more foam production. Surfactant solutions did reduce oxygen transfer but the magnitude of the decrease was surfactant dependent.

Downing, *et al.* (1960) showed the addition of 5 mg/L SAA increased the oxygenation capacity for mechanical aerator systems. An addition of a liquid antifoam agent to the surfactant solution decreased the oxygen absorption coefficient by 11%. Schmit, *et al.* (1978) used 5 mg/L of a linear alkylbenzene sulfonate (LAS) and observed large volumes of foam. The measured LAS concentration before and after each test showed substantial decreases in concentration which they attributed to losses in the foam fraction. They also observed changes in $K_L a$ with LAS additions.

2.4.2   Alpha, Beta and Theta Factors

The oxygen transfer equation is:

$$\frac{dC}{dt} = K_L a (C_\infty^* - C) \qquad (7)$$

where:

$$C \quad = \quad \text{dissolved oxygen concentration;}$$

$$K_L a \quad = \quad \text{overall oxygen transfer coefficient;}$$

$$C_\infty^* \quad = \quad \text{dissolved oxygen concentration at infinite time.}$$

Integrating Equation 7 with the conditions at $t = 0$, $C = C_o$ leads to:

$$C = C_\infty^* - (C_\infty^* - C_o)e^{K_L a t} \tag{8}$$

The recommended method to estimate the parameters $K_L a$, C_∞^*, and C_o is the linearization technique (Stenstrom, *et al.*, 1981) on the exponential form using unsteady-state test data. The unsteady-state clean/process water testing should be performed under the formalized guidelines set by the ASCE Committee on Oxygen Transfer (1984). The guidelines insure increased uniformity in testing, thus insuring the reliability of test results.

The clean/process water parameters are related to α, β, and θ. These parameters are used to relate the oxygen transfer rate (OTR) in the field to the standard oxygen transfer rate. Standard oxygen transfer rate (SOTR) is defined in the United States as the amount of oxygen transferred to tap water at 20°C with zero initial dissolved oxygen concentration under 760 mm Hg barometric pressure and at 36% relative humidity. OTR is related to SOTR by:

$$OTR \quad = \quad \alpha \left(\frac{\beta C_\infty^* - C_L}{C_\infty^*} \right) \theta^{T-20} SOTR \tag{9}$$

$$\alpha \quad = \quad \frac{K_L a_{PW}}{K_L a_{TW}} \tag{10}$$

$$\beta \quad = \quad \frac{C_{\infty PW}^*}{C_{\infty TW}^*} \tag{11}$$

$$\theta^{T-20°C} \quad = \quad \frac{K_L a(T°C)}{K_L a(20°C)} \tag{12}$$

where:

$K_L a$ = volumetric mass transfer parameter;

C_∞^* = saturated dissolved oxygen concentration;

PW   = subscript indicates process water;

TW   = subscript indicates tap water;

$K_L a(T)$ = $K_L a$ at temperature T;

C_L = desired dissolved oxygen concentration.

These parameters were discussed in detail in Stenstrom and Gilbert's (1981) review paper. These is no concensus value assigned to any of the empirically determined parameters; however, the value of 1.024 for θ at systems close to 20°C has reached acceptability. The β factor is determined by the Winkler test if there is no test interferences. This factor is normally close to unity.

When the experimental design remains unchanged to estimate the parameters, θ is a function of temperature and α and β are functions of fluid properties. θ and β yield fairly consistent values regardless of aeration technique, although θ was shown to be affected by the degree of turbulence (Hunter, 1979). α is dependent on the aeration system.

The importance of estimating α and β has been shown (Stenstrom and Gilbert, 1981). The error profile they calculated for the given situation ($C_\infty^* = 2$, $\alpha = 0.8$, $\beta = 0.9$, T = 18° C, and $\theta = 1.024$) showed for a 10% error in α and β, the error in predicting the field OTR was 20%.

A goal of α testing is to make α dependent only on wastewater properties and not on basin geometry or aeration type. British researchers (Lister and Boon, 1973) have had some success in this area by performing the clean water test with tap water plus 5 mg/L anionic surfactant. The surfactants simulate the effect of

42

wastewater contaminates on oxygen transfer. They define α to be:

$$\alpha_S = \frac{K_L a_{PW}}{K_L a_{TW+S}}$$ (13)

where:

$K_L a_{TW+S}$ = K_La of tap water with surfactants.

The resulting values of α_S appear to be less dependent on aerator type, thus closer to ideal. Their modified α_S factors are closer to unity so there is less error in scale-up.

2.4.3   Summary

This section first summarized the oxygen transfer process in diffused aeration. The effect of surfactants on the transfer process was discussed. Finally, the parameters describing the field oxygen transfer rate with the standard oxygen transfer rate were presented.

Chapter 3

Experimental Design

3.1 Dynamic Surface Tension Apparatus

The literature review of various surface tension measuring techniques showed the maximum bubble pressure method to be the optimal dynamic surface tension measuring technique based on costs, measuring accuracy, and ease of construction. The design selected for this research is patterned after Bendure's (1971) work.

The bubble formation process (Figure 2) begins with water flow from the constant head reservoir, through a rotometer, and into a water trap chamber which forces air out as the new working fluid. After passing through a desiccator, the air releases through a submerged glass capillary tip forming bubbles in an aqueous solution. An inclined manometer visually monitors the system's pressure. A differential pressure transducer's signals connects to a personal computer utilizing Labtech Notebook software to record data. Another pressure transducer monitors relative changes in barometric pressure during an experimental run.

The bubbling process begins with pressure accumulation to overcome static
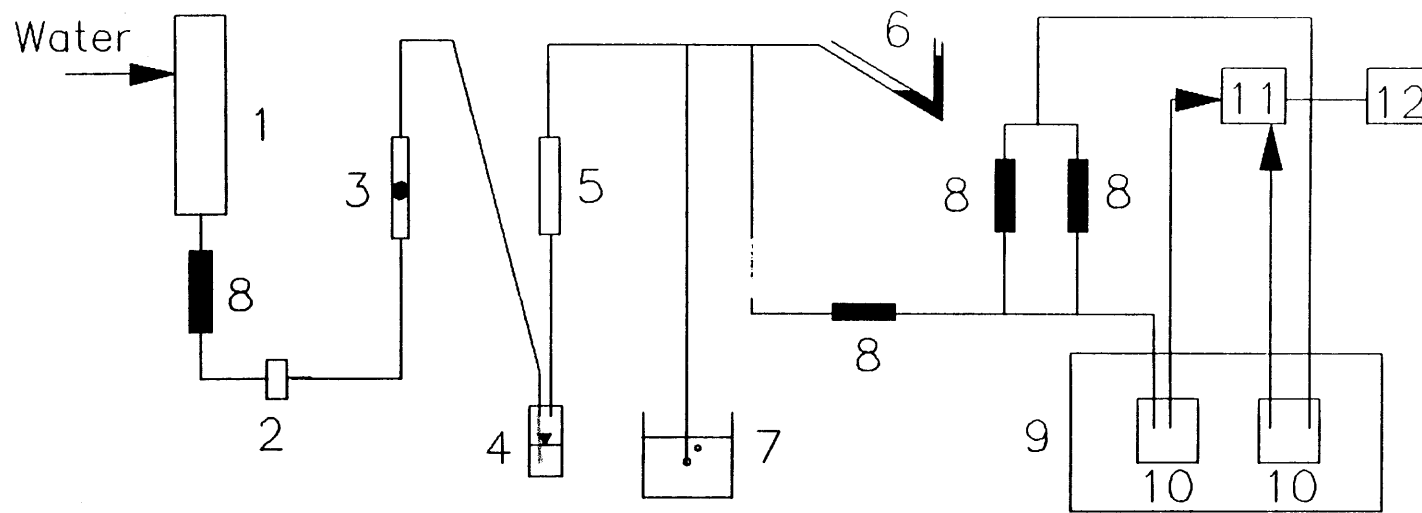
1. constant pressure head   7. beaker
2. needle valve   8. ball valves
3. rotometer   9. water bath
4. catchment   10. large-volume vessels
5. dessicator   11. pressure transducer
6. manometer   12. recorder

Figure 2:   Dynamic Surface Tension
Measuring Device

head and friction losses. Bubbles are not formed during this period which takes from a few seconds to 15 minutes, depending on the flow rate. The static head loss (capillary immersion depth) is measured with a wire hook attached to a vernier caliper (± 0.005 cm). The wire hook, raised from below the water surface, dimpled, and thus located the surface. The friction losses were calculated on a daily basis.

Bubble formation and release can be described as a series of spikes on the strip chart (Figure 3). The voltage output are changed to pressure readings through daily transducer calibration checks. The maximum bubble pressure is the recorded bubble pressure minus a friction factor. Figure 3 is typical representation of the data collected for one point on the dynamic surface tension measurement (DST) curve. Bubble formation time (bubble life) is taken as the averaged time interval between successive peaks with the corresponding surface tension value the averaged value of those peaks for that flow rate. The flow meter and the needle valve regulate the flow rate to construct a wide range of bubble lives to form the DST curve.

Outside influences (such as barometric pressure and temperature changes) affect the surface tension measurement during the life of one bubble because after the bubble detaches, the system returns to its pre-bubble state. Although the experimental set-up is not complex, the sensitivity of the system and its response to external excitations posed a few problems.

1. Sensitivity of equipment. The pressure required to form a bubble was dependent on capillary tip radius and the fluid surface tension. The pressure values observed in this study were about 0.5 inch of H_2O (0.0185 psi). The pressure transducer used to measure the bubble pressure had a range of 0.0 inch - 1.0 inch of H_2O. Such sensitivity required the utmost care and accuracy in measurement technique and precision equipment.

46
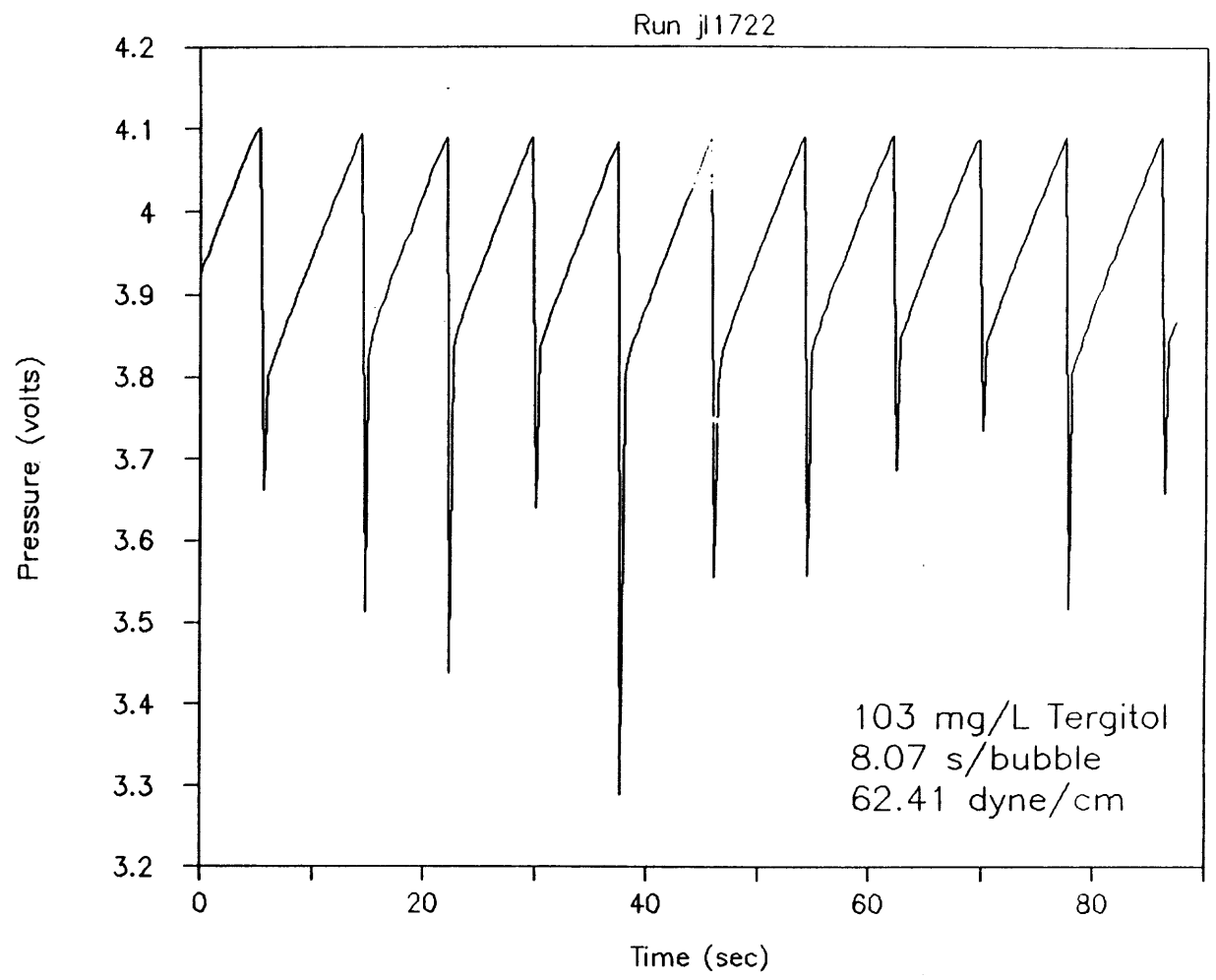
Figure 3: Typical Bubble Formation Pattern

2. Temperature. According to the ideal gas law, all variables remaining constant, a temperature increase of 0.7°C corresponds to a pressure increase of0.1 inch of H_2O. Slight temperature fluctuations on the overall system affect pressure readings. To reduce environmental interferences, large volume air reservoirs are submerged in an unregulated water bath. The large water mass kept the temperature fluctuations to a minimum. The daily temperature variation, observed as noticeable drift because of the vapor pressure changes in the water trap, was eliminated by installing a moisture trap.

3. Back pressure. The air reservoirs served a dual purpose of reducing back pressure from the diaphragm pressure transducers. As differential pressure is applied across the diaphragm, the air displacement from that movement, if inhibited by short transmission lines, is enough to induce serious error from true differential pressure. The short transmission lines create back pressure whereby the more positive pressure applied across the diaphragm, a smaller incremental change is reflected in the transducer readings. The displaced air must be released into a large-volumed vessel to reduce this effect.

3.2 Sensitivity Analysis for Pressure Head

A sensitivity analysis was used to determine the magnitude of perturbations in the measured parameters on surface tension values. The effects listed in Table 4 deviate from the control situation of: 0.55 inch of H_2O pressure head, 0.2 cm H_2O static head, and 0.99823 gm/cm^3 water density at 20° C. The greatest changes in surface tension are associated with changes of ±0.1 inch of H_2O in the head measurement and ±0.1 mm H_2O in the static head measurement.

48

Pressure Head	Static Head	Surface Tension	$\Delta 50.01 - \gamma_i$	Deviations from Control
0.55	0.2	50.01	0.0	control
0.5501	0.2	50.02	-0.01	+0.0001 pressure head
0.551	0.2	50.11	-0.01	+0.001 pressure head
0.56	0.2	51.03	-1.02	+0.01 pressure head
0.65	0.2	60.9	-10.89	+0.1 pressure head
0.55	0.19	50.41	-0.4	-0.01 static head
0.55	0.3	45.42	4.59	+0.1 static head
0.55	0.2	50.01	0.0	+1°C temperature
0.55	0.2	50.01	0.0	+2°C temperature

Table 4: Sensitivity Analysis for Pressure Head

The manually determined static head measurement is a potential source of large error and was; therefore, carefully measured and checked. The ±0.005 cm accuracy of the vernier represents minor error if read incorrectly. Pressure transducer values are unlikely sources of error because they were calibrated daily and operate with no manual interferences. All other losses/gains are within acceptable experimental error.

3.3 Equations for Surface Tension

Sugden's development of the maximum bubble pressure measurement for surface tension is outlined below. The measurement is a function of the capillary radius, surface tension of the fluid, and the density differential across the interface (Figure 4).

Pressure at point O (Figure 4) in excess of pressure at point t is given by:

$$P_o = \frac{2\gamma}{b} + \Delta\rho g z \qquad (14)$$
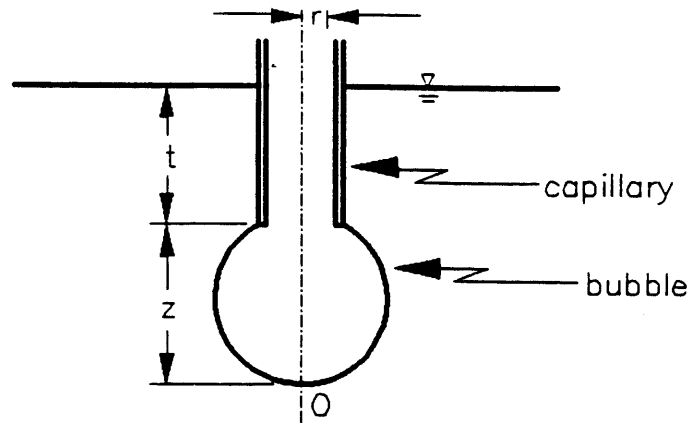
Figure 4: Bubble Pressure Measurement

where:

$$\Delta\rho \quad = \quad \rho_l - \rho_g$$

$$\rho_l \quad = \quad \text{liquid density}$$

$$\rho_g \quad = \quad \text{gas density}$$

The first term on the right hand side of Equation 14 is the surface tension term after the Young-Laplace equation. It is assumed at $z = z_{max}$, (point O), b $= R_1 = R_2$; the radii of curvature at O is equal to some value b, not necessarily the capillary radius. The second term on the left hand side of Equation 14 is the hydrostatic pressure where z varies from 0 to z_{max}. It can be simply stated:

$$P_o = P_{max} - P_t \tag{15}$$

or:

$$P_o = \Delta\rho g h \tag{16}$$

50

where:

P_{max} = reading from the transducer;

P_t = hydrostatic pressure at depth t;

h = head to form bubble.

Various substitutions transform Equation 14 into:

$$\frac{r}{X} = \frac{r}{b} + \frac{r}{a}\frac{z}{b}\left(\frac{\beta}{2}\right)^{1/2} \qquad (17)$$

where:

β = $\frac{2b^2}{a^2}$ = $\Delta\rho g\frac{b^2}{\gamma}$

X = $\frac{a^2}{h}$

a^2 = $\frac{2\gamma}{\Delta\rho g}$ = rh = capillary constant

Sugden derived a table of minimum values of $\frac{X}{r}$ for $0 < \frac{r}{a} < 1.5$. This table incorporated the parameters β, $\frac{z}{b}$, and $\frac{r}{b}$ so the capillary constant becomes the equation of interest. Since a^2 is a function of surface tension, a trial and error solution is required:

1. Assume X = r.

2. Calculate $a^2 = Xh$.

3. Calculate $\frac{r}{a}$. From this value, find the corresponding $\frac{X}{r}$ value from Sugden's table.

4. Calculate a new X' value.

5. Calculate $a^{2'} = X'h$.

6. Compare $a = a'$ to Step 1 and iterate until $a = a'$.

7. Calculate surface tension.

A simple computer program, with Sugden's table stored in memory, was used to calculate surface tension. The values of $\frac{X}{r}$ were calculated from linear interpolation.

3.4 Aeration Apparatus

The aeration studies were performed (Figure 5) in a 55-gallon tank with baffles using two fine bubble diffuser stones. Two dissolved oxygen meters and probes were used to measure the dissolved oxygen in the tank. The probes were calibrated before each use by the Winkler-Azide modification method.

The water was deoxygenated by a combination of nitrogen stripping and cobalt-chloride-sodium sulfite reaction to keep the dissolved solids concentration low. Water was replaced in the tank before the dissolved solids concentration reached 1500 mg/L. The solids concentration was monitored via conductivity measurements after establishing a strong correlation of the form:

$$TDS = 48.567 + 0.7065(Cond) \tag{18}$$

Equation 18 was calculated with a correlation coefficient (R^2) of 0.988. The dissolved oxygen meters were connected to a linear strip chart recorder for monitoring and permanent record. Selected values from the recordings were used to estimate $K_L a$, C_∞^*, and C_o by the exponential technique (Stenstrom, $et\ al.$, 1981). The $K_L a$ value representative of the run was the averaged value from the two probes.

52

28" 34" 36"

22"

2.2"

Manometer

Rotometer

DO Meter

DO Meter

Air Supply

55—gal Aeration Vessel

Recorder

C vs t data
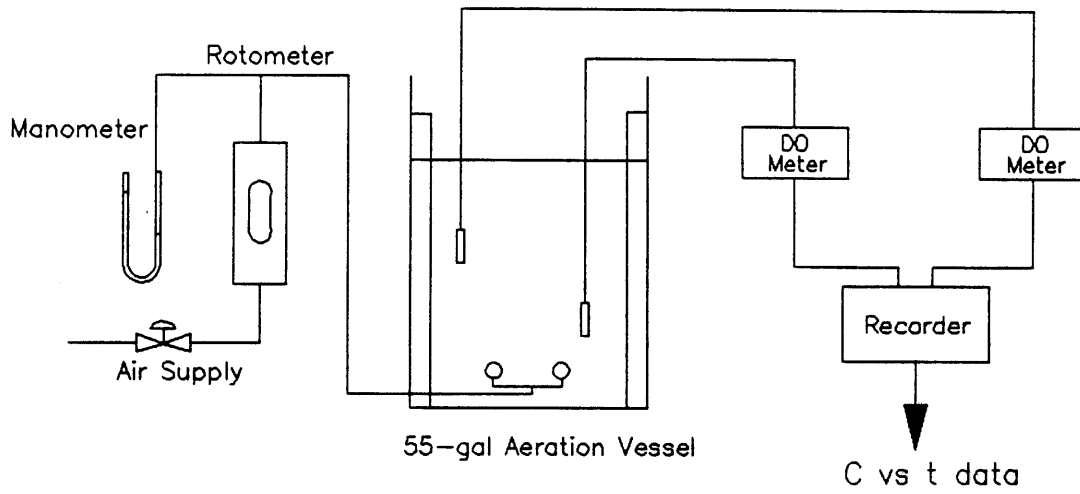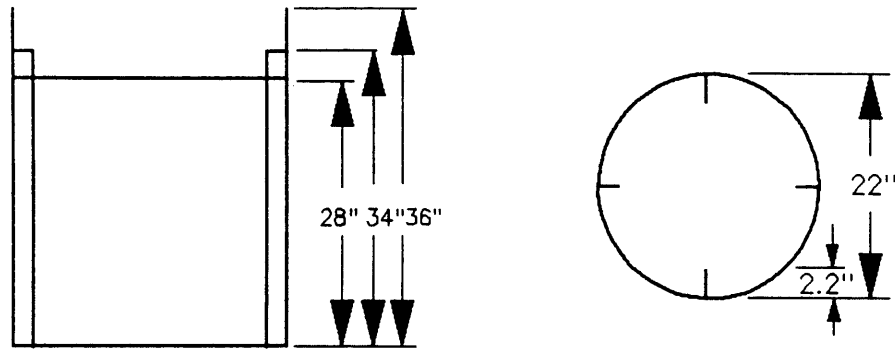
Figure 5: Aeration Equipment

3.5 Surfactants

Dodecyl sodium sulfate (DSS) and tetradecyl sodium sulfate (under the Union Carbide trade name of Tergitol 4) were the surfactants chosen for this study (Table 5). DSS is a well-known surfactant that has been used in aeration and DST studies. Tergitol has also been used in aeration studies.

3.6 Bubble Diameter Measurement

A clear acrylic 1 ft × 1 ft × 3 ft box was used as an aeration vessel to determine bubble sizes. Bubbles formed in clean water and surfactant solutions were photographed using a 35 mm SLR camera fitted with a 50 mm macro lens. Photographed in each slide was a ruler with a 0.01 inch graduations as a reference measurement. Bubbles were successfully captured at a shutter speed of 125th with an automatic electronic flash for each flow rate.

Bubble diameters were measured from projected slide images with suitable correction factors for its enlargement. All bubbles in an 1 inch square template were measured from a 2× enlargement. The slides were shot at the middle of the column at the same depth the DST samples were retrieved in the aeration tank so the bubble size would correspond to the DST measurement. Major and minor radii of ellipsoidal bubbles were measured and such bubbles identified by radius of spheres having the same volume as the ellipsoidal bubble. Depending on the bubble sizes, an average of 36 bubbles per square were measured for the surfactant solutions and an average of 12 bubbles per square were measured for tap water.

Table 5. Surfactants

	Dodecyl Sodium Sulfate	Tetradecyl Sodium Sulfate
Chemical Formula	$CH_3(CH_2)_{11}O\ SO_3N_a$	$CH_3(CH_2)_{13}O\ SO_3N_a$
Formula Weight	288.38	316.43
Critical Micelle Concentration (M)	T=40°C 8.6×10^{-3} T=25°C 8.2×10^{-3}	T=40°C 2.2×10^{-3}
Effectiveness of Adsorption	T=25°C $3.4 - 3.6 \times 10^{10}$moles/cm^2	
Area/Molecule at Surface	49 - 46Å	
Surface Tension		T=25°C 56.6 dyne/cm

Data taken from Rosen (1978) *Surfactants and Interfacial Phenomena*, John Wiley & Sons, New York, New York.

3.7 Calculation of Terminal Rise Velocity

The surfactant bubbles were identified as spherical-shaped particles. The air bubbles in water were more ellipsoidal and irregular. The following equation was used to calculate terminal rise velocity:

$$u_t = \sqrt{\frac{4gD(\rho - \rho_p)}{3\rho C}} \qquad (19)$$

where:

u_t	=	terminal rise velocity;
g	=	gravitational constant;
D	=	bubble diameter;
ρ_p	=	particle density;
ρ	=	fluid density;
C	=	drag coefficient.

The drag coefficient was calculated as (Metcalf and Eddy, 1979):

$$C_D = \frac{24}{Re} + \frac{3}{\sqrt{Re}} + 0.34 \qquad (20)$$

where Re is the Reynold's number. The resulting terminal rise velocities were slightly higher than those found by Haberman and Morton (1953) in tap water. A computer program calculated the terminal rise velocity using an iterative technique and a stopping criterion of 1.0 in Re.

3.8 Sensitivity Analysis of Radius Size

A sensitivity analysis was performed to determine the effect of the measured bubble radius on K_L. The results in Table 6 show a ±10% change in the control

diameter (inch)	radius (cm)	vel (cm/s)	Re	area	K_L (cm/hr)	ΔK_L	
0.0385	0.048895	12.54	121.83	41425.878	14.975814		control
0.0435	0.055245	13.97	153.28	32911.246	18.850281	-3.87446	+10%
0.03465	0.044005	11.4	99.63	50631.629	12.252939	2.722874	-10%
0.04427	0.056222	14.17	158.32	31882.371	19.458598	-4.48278	+15%
0.03273	0.041567	10.86	89.72	56267.052	11.025746	3.950067	-15%

Table 6: Sensitivity Analysis for Bubble Diameter

radius led to a 18-25% change in K_L. It appears a small error in measuring the bubble radius can lead to an erroneous K_L value; therefore, careful measurement of the bubble is required to insure representative K_L values. The values used in this study were the averaged values taken from at least three photographs and were generally within 10% of the mean. In addition, more than 10 bubbles were measured in each photograph.

3.9 Calculation of K_L

The total surface area was calculated as follows for each flow rate:

Total # of bubbles formed $N_b = \frac{Q}{(4/3)\pi r^3} 1000$

Total surface area per unit time $N_b 4\pi r^2 = \frac{3Q}{r}$

Depth of water diffusers 63.5 cm

Retention time $t = 63.5/\text{vel of rise}$

Total surface area $A_{total} = \left(\frac{3Q}{r} \frac{63.5}{vel}\right)/60$

57

K_L is given by:

$$K_L = K_L a \frac{V}{A_{total}}$$ (21)

Chapter 4

Results

The results of this research are partitioned into three sections. The first section verifies that the constructed DST measuring device yields accurate values of surface tension within the limitations and expectations of the design. Preliminary results on surfactant aeration testing are discussed in the second section. The third section correlates oxygen transfer with DST measurements.

4.1 Equipment Verification

4.1.1 Friction Factor

The first experiments using the DST measuring device were performed on tap and bottled water. Pure water has a surface tension value of 72.75 dyne/cm at 20°C (Harkins, 1952), any deviation from this measured value using the DST device is attributable to experimental errors such as the effects of headlosses (friction) and are collectively termed "friction factor" (ff). The deviation in the measured surface tension from the known surface tension of pure water was estimated from

measurements over representative bubble times.

$$\text{ff} = \frac{\Sigma 72.75 - \gamma_i}{n} \qquad (22)$$

where:

γ_i = surface tension value obtained by DST device at flow rate i;

n = total number of runs.

The friction factor was calculated on bottled drinking water. Equation 22 uses the pure water surface tension value as a reference. Although bottled drinking water is not pure water, this substitution was an affordable compromise that yielded more consistent results than with tap water. If experimental conditions remained fixed, the friction factor should be fairly constant, but this was not the case (Figure 6). The friction factor, which was determined at the start of each days' experiments, showed day-to-day variations, indicating extraneous influences affected the DST measurements. No correlations were found for the friction factor with capillary depth or with water temperature. From the magnitude of the observed bubble pressures, the daily changes in barometric pressure may interfere with the pressure transducer readings and thus, could cause the observed fluctuations in the friction factor. This possibility warrants further investigation.

The friction factor correction determined at the beginning of each day was averaged over the range of bubble formation times. As expected from fluid mechanics, at lower flow rates (long bubble life) the headloss difference $(72.75 - \gamma_i)$ is lower, indicating a reduction in headloss due to velocity friction. This reduction is small compared to the average value so is not treated separately (Figure 7).

The friction factor was in the range of ± 3 dyne/cm, which is about 4% of the static surface tension value of water. This correction factor was applied to all observed DST measurements taken durng that day in an attempt to minimize the
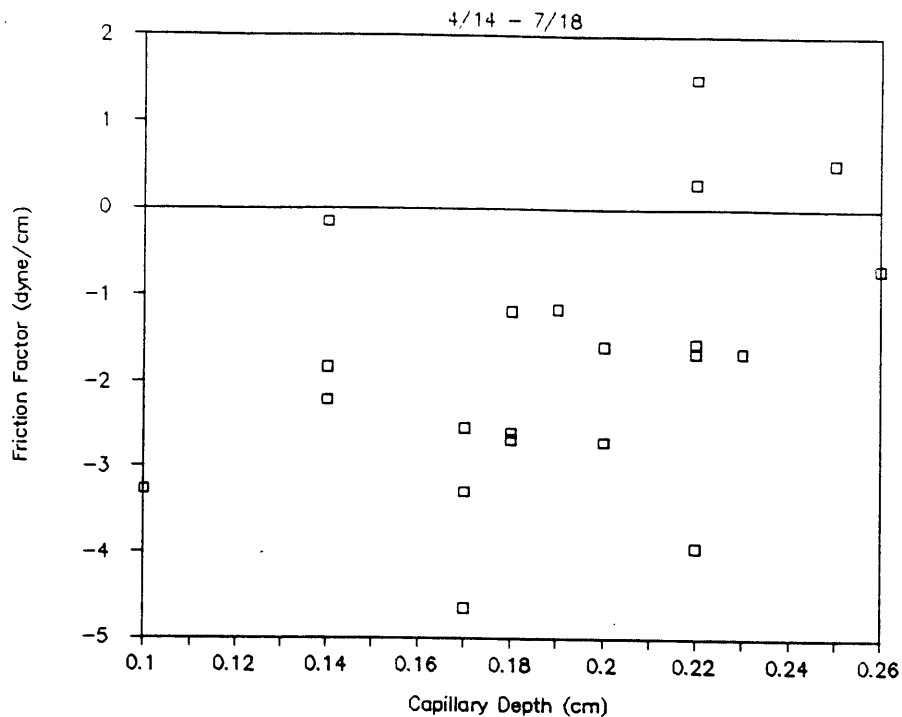
Figure 6: Friction Factor vs. Capillary Depth

day-to-day observed variations in the DST data obtained under similar conditions.

4.1.2 Dynamic Surface Tension Function and Model

The dynamic response of a surfactant on surface tension is shown in Figure 8. Surfactants decrease surface tension values with increasing bubble age because more time is allowed for surface adsorption. Similarly, lower surface tension values for the same bubble life at higher surfactant concentrations results from more surfactants adsorbing at the interface, as indicated by steeper DST curves.

An equation to describe the data was developed by an observation in Bendure's formulation (1981). He presented two diffusion-controlled adsorption equations relating DST measurements to bulk surfactant concentrations and to bubble life.
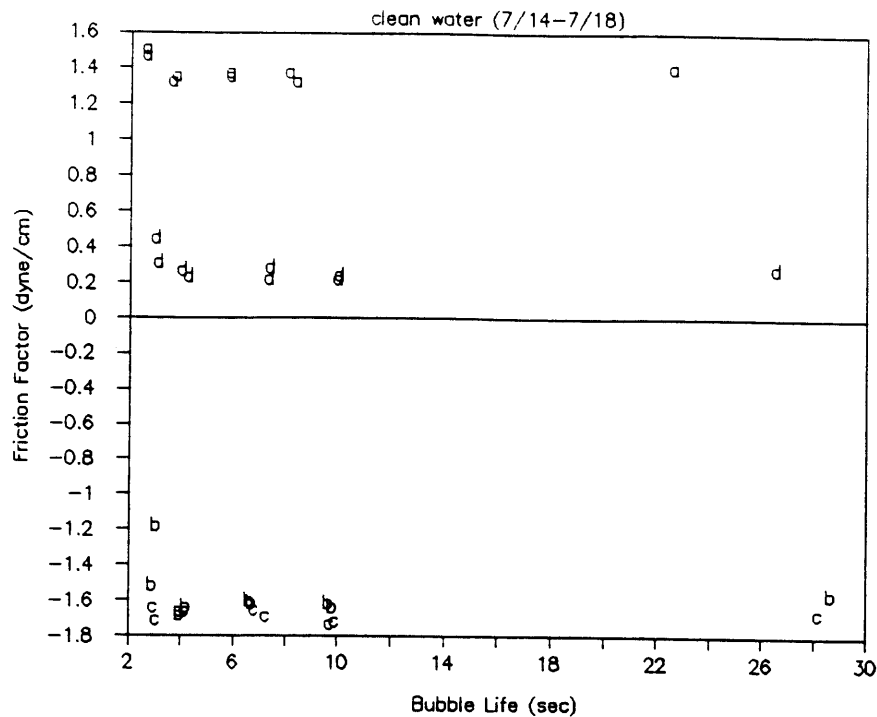
Figure 7: Friction Factor vs. Bubble Life

For long adsorption times, > 2.8 sec, which obey Langmuir isotherms:

$$\gamma - \gamma_\infty = \frac{\Gamma_m^2 RT}{\sqrt{\pi \overline{D}} C_o \sqrt{t}}$$

The subsequent model used to describe the experimental data is:

$$\gamma - \gamma_\infty = \frac{X}{C_o \sqrt{t}} \tag{23}$$

where X is the lumped parameter (slope) encompassing the surface excess concentration and the diffusion coefficient. By calculating the variable $\frac{1}{C_o \sqrt{t}}$ for all experimental conditions, linear least squares can be used to estimate the infinite-time surface tension value (γ_∞) as the intercept and the X parameter as the slope. Figure 9 shows the fit between the model and the actual data for one experiment.

The "correctness" of the model fit to the data is demonstrated by the coefficient of determination. The results of 45 data sets of Tergitol solutions are presented in
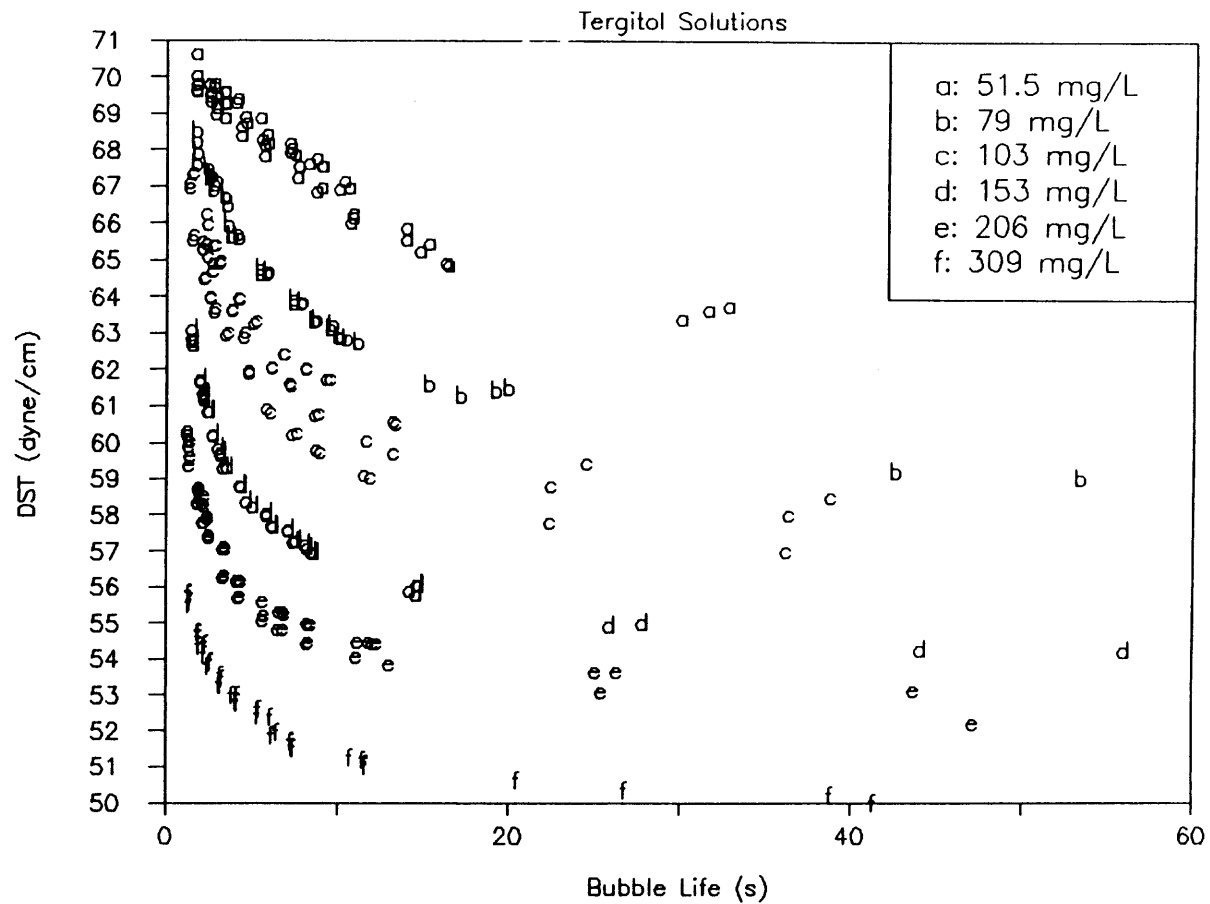
Figure 8: DST Curves for Tergitol Solutions

March 08, 1988 run 92

Tergitol data subset #7
100 mg/l
X = 1815
inter = 56.71 dyne/cm
R-square = 0.993

bubble life

a   real values   ———— calculated values
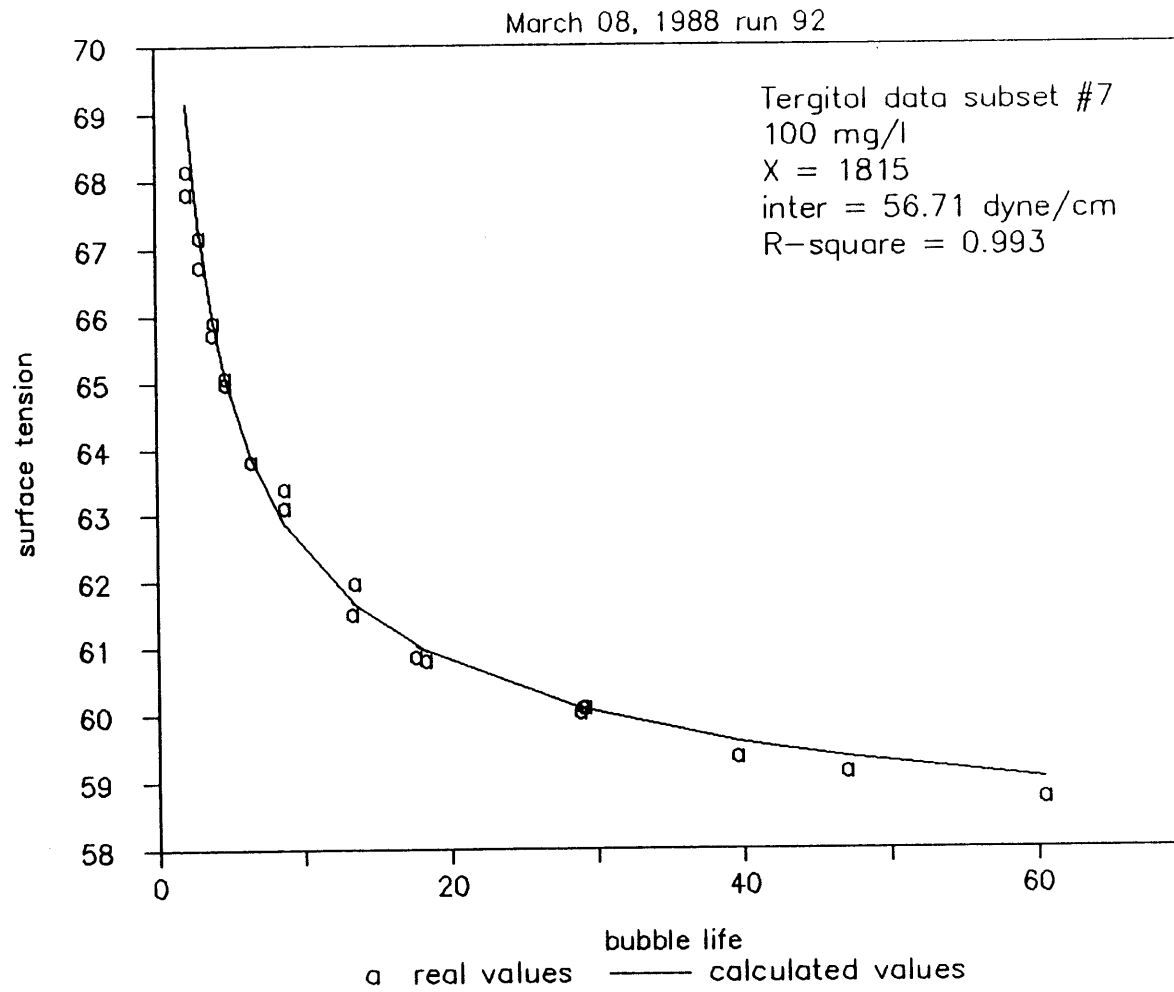
Figure 9:   Model Fit

R-squared	number	concentration
0.98-1.0	18	
0.96-0.98	3	
0.94-0.96	1	100
0.92-0.94	2	
0.90-0.92	-	
0.88-0.90	7	
0.86-0.88	5	
0.84-0.86	5	50
0.82-0.84	4	

Table 7: Model Fit R^2 for Tergitol Solutions

Table 7. The high concentration data set show greater correlation than the lower concentrations, indicating the model fits steeper functions. All the correlation coefficients are greater than 0.82.

An analysis of X vesus the measured static surface tension value (by the du Nouy ring tensiometer and hereafter referred to as "duNouy") is shown in Table 8 and Figure 10. Figure 10 indicates higher surfactant concentrations correspond to greater X parameter values as expected from adsorption theory. It is more probable at high surfactant concentrations more surfactant molecules will adsorb at the interface than at low surfactant concentrations for the same period of time. More surfactants at the surface results in lower surface tension values, steeper DST curves and higher X values.

Another indicator of the "correctness" of the model is the correlation between the intercept of the linear model (parameter name: inter) and the duNouy measurement. The intercept of the model is the infinite time surface tension value (γ_∞) which should be the equilibrium surface tension value, $i.e.$, the duNouy measurement. Table 8 and Figure 11 indicate this concept is valid.

non-aerated solutions

X
(Thousands)

4.5 —
301.6
4 — 301.6
301.6
3.5 — 200.3
200.3
200.3
3 — 200.3

Tergitol

2.5 — 309
309

2 — 153
206 153
100.8 206 153
100.8 103
100.8 103 103
1.5 — 78.6 78.6

74
74
DSS
53 53
1 —
53

55 51.5

0.5 —

38   40   42   44   46   48   50   52   54   56   58
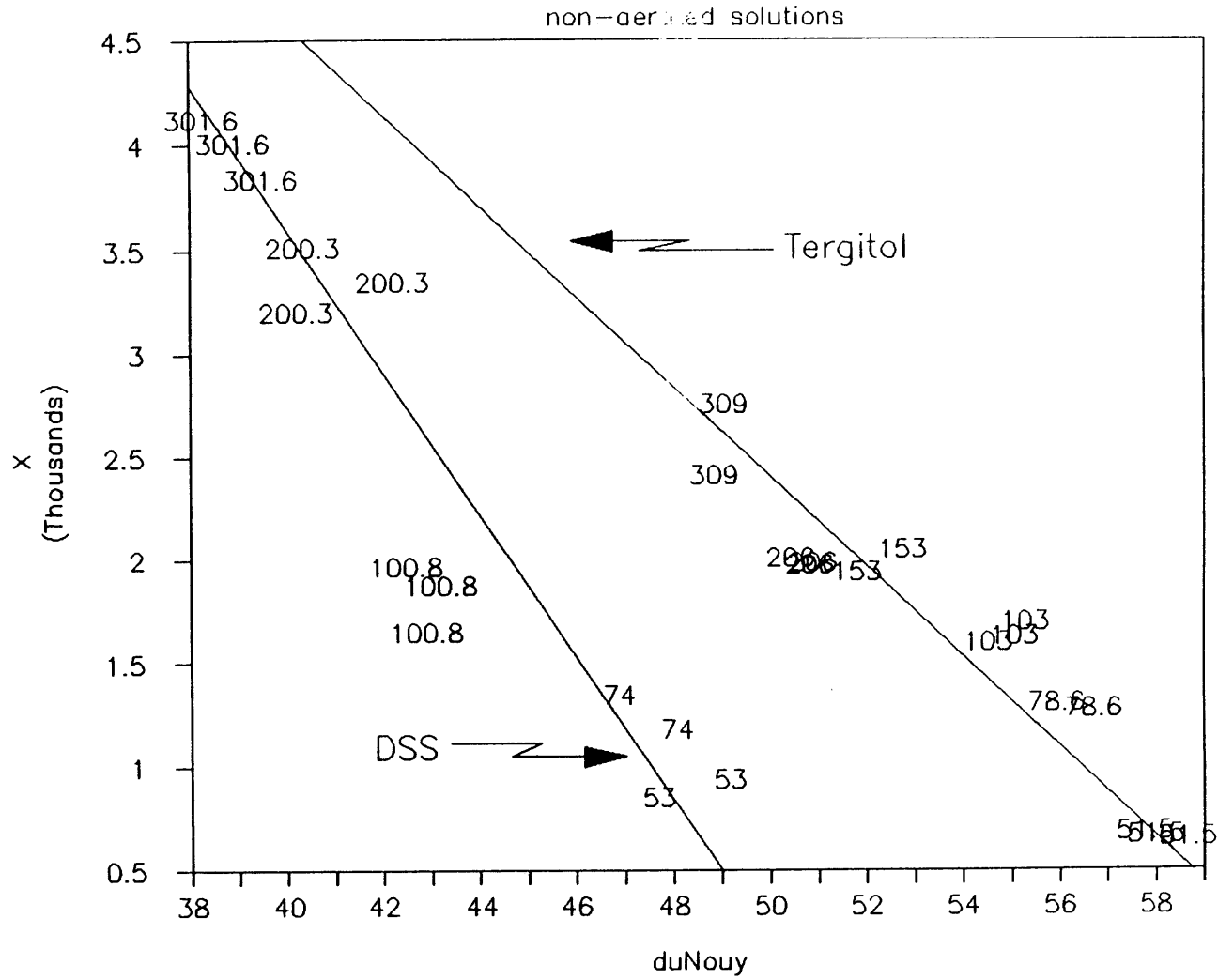
duNouy

Figure 10: X vs. DuNouy
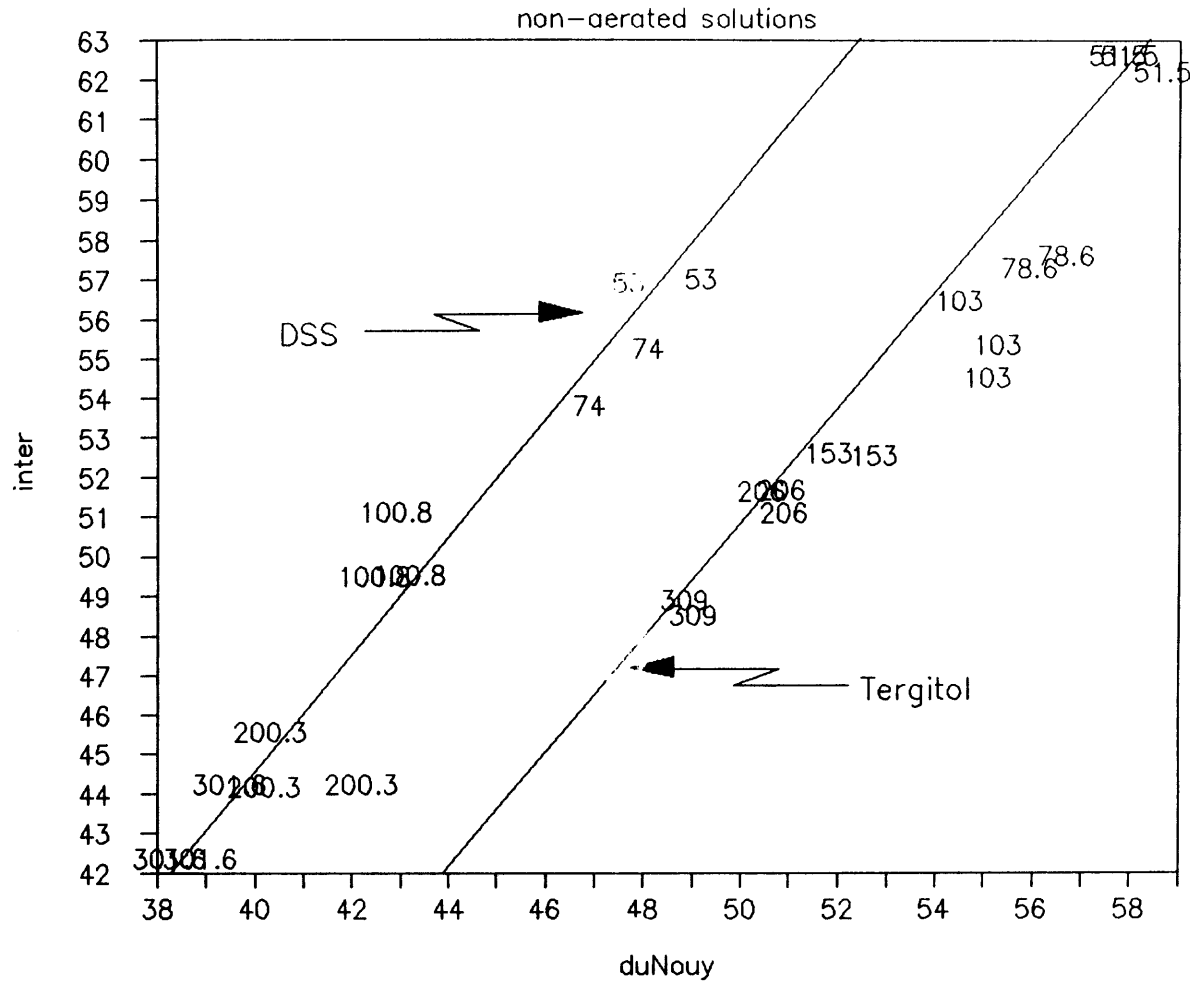
Figure 11:   Inter vs. DuNouy

γ_∞ vs. duNouy		
Results	Tergitol	DSS
intercept	-18.13	-12.04
slope	1.361	1.416
R^2	0.926	0.932
X vs. duNouy		
intercept	1233	15811
slope	-178.44	-310.41
R^2	0.896	0.873

Table 8: Correlations from duNouy Measurements

This model was chosen over:

$$\gamma - \gamma_\infty = \frac{X'}{\sqrt{t}} \tag{24}$$

where $X' = \frac{X}{C_\circ}$. This simplification of the slope, X, increases the utility of the DST measurement because information regarding the initial surfactant concentration is unnecessary to calculate X' and γ_∞. Initial surfactant concentration information will never be available for process water conditions; therefore, some pseudo concentration must be selected if DST measurements are to be useful under process conditions. Determining a parameter to estimate the surfactant concentration requires further investigation. Even with the surfactant concentration complication, Equation 23 was chosen because the model residuals, plotted over bubble life, were more random than those of Equation 24 whose residuals showed a distinct lack of fit.

4.1.3 Bubble Life vs. Flow Rate

The data in Figure 12 show the reproducibility of the DST measurements. The variation of bubble life with flow is a reflection of the surface tension of the
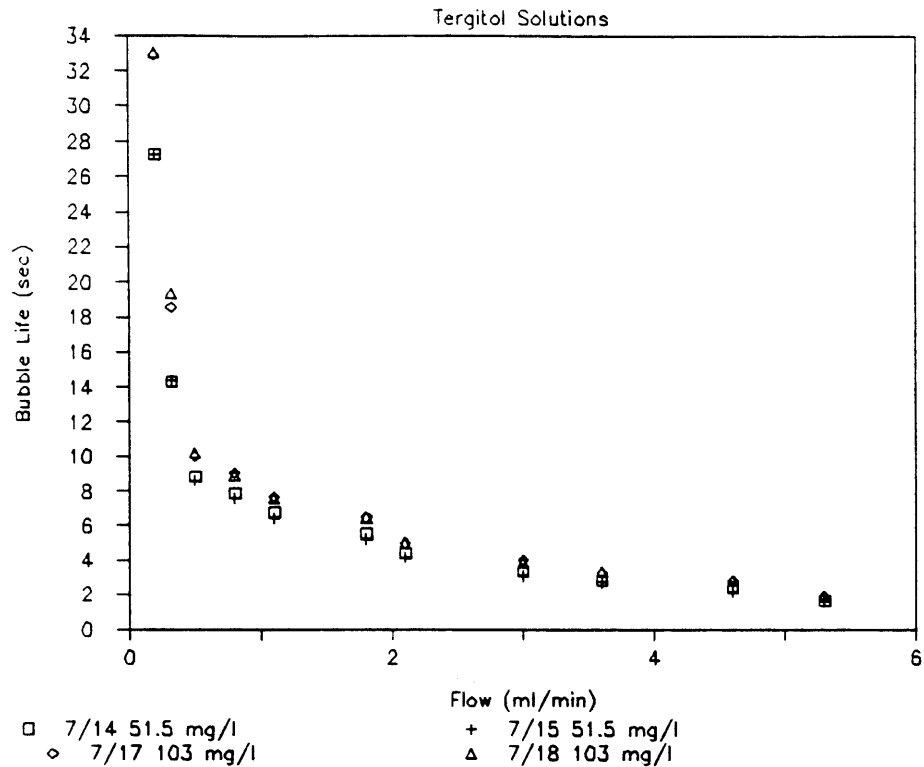
Figure 12: Bubble Life vs. Flow

liquid. At the same flow rate, the higher Tergitol surfactant concentrations have longer bubble lives than the low surfactant concentrations. More surfactants in the bulk solutions compete for the active adsorption sites; therefore, for the same time interval, more surfactants are expected at the interface to decrease surface tension. The decrease in surface tension, corresponds to increased elasticity of the surface; hence, greater shear force is required to detach the bubble, resulting in longer bubble lives.

Figure 12 also shows the consistency in bubble life times for each flow rate and concentration. This is a typical result for surfactant solutions.

4.2 Preliminary Aeration Results

4.2.1 Surfactant Concentration Gradients

The observation of changing mixing patterns (Hwang and Stenstrom, 1979) in the aeration basin with changing surfactant concentrations has led to speculation of the existence of surfactant gradients in the mixing patterns. Until recently, there has been no method to verify this type of observation; however, the DST measurement is able to detect surfactant concentration gradients in the aeration vessel. Visual evaluation of the DST curve or calculated X values reflect the apparent differences in surfactant concentrations between samples taken from the top and bottom of the tank. As shown previously, the higher X values, corresponding to a steeper DST curve, indicate higher surfactant concentration.

Table 9 summarizes the results of DST calculations on the top and bottom samples of 200 mg/L Tergitol solutions aerated under various flow rates. A cut-off level of a 4% difference between the mean of the top and bottom measurement was the criterion used to determine placement in the categories.

The majority of the samples fall into the "no change" category indicating the apparent lack of surfactant gradients. This complete mix condition may be the result of the shallow water depth of the test vessel and high air flow rates. The lack of conclusive surfactant gradient patterns in the aeration tank may also be attributed to changing mixing patterns in the tank. Hwang and Stenstrom (1979) noted two different water circulation patterns for identical surface aeration designs at the same surfactant concentrations. For certain conditions the top-to-bottom patterns would shift to top half and bottom half cell circulation patterns with no interactive mixing for minimum changes in mixing energies. This observed

aeration flow rate	$X_b > X_t$	$X_b < X_t$	no change	total
20000 L/min	2	2	3	7
12000 L/min	3	2	2	7
8050 L/min	3	2	8	13
6050 L/min	1	2	4	7
*at 4% from mean difference between top and bottom				

Table 9: Surface Tension Gradient Investigation

phenomenon may explain why surfactant gradients exist between the top and the bottom of the tank but no pattern was established for the direction of the concentration gradient as a function of flow rate. What has been established, is the use of DST to detect apparent surfactant concentration differences.

Although these conclusions are applicable only to this aeration design, some form of surfactant concentration gradient is expected for most basin geometries and aeration techniques. Careful investigation of possible sampling sites is needed to obtain representative X values and must be obtained from the same circulation patterns. A mid-depth sampling site was selected for this aeration design.

4.2.2 Foaming and Repeated Aeration Experiments

As aeration experiments are repeated in the test tank without changing the water or adding fresh surfactant, $K_L a$ increased (Figure 13). This phenomenon can be explained by surfactant deterioration or a gradient in surfactant concentration caused by foaming (Burgess and Wood, 1959; Ewing, *et al.*, 1979). As repeated experiments are performed on a solution, the foam changes in character and quantity. An early foam appears as light and airy (large entrapped air bubbles), whereas after repeated runs, the foam becomes dense and compact (very

small entrapped air bubbles). The changing foam characteristics may indicate surfactant deterioration which indicates an effective concentration of SAA that is less than the stated concentration. This may account for the increasing K_La values because water containing lower surfactant concentrations have higher K_La. The foam character changes may also indicate more surfactants are being drawn from the test solution into the foam. Support for these theories is based on the observation as the number of experiments with the same test solutions increased, there was a general trend in corresponding decreases in X. The decrease in X translates to a decrease in surfactant concentration in the test solution.

Foaming of DSS solutions increased the difficulty in accurately determining K_La at a particular solution concentration. Not only did K_La increase with almost every test, but during the course of 4 or 5 repeated experiments, the range of K_La increase was significant. Increasing K_La suggests careful experimental procedures must be observed when performing repetative experiments. The initial surfactant concentration in the aeration basin may no longer be the actual surfactant concentration after four or five experiments. The corresponding measured K_La for each experiment should be correlated with the actual surfactant concentration, not the initial concentration. If K_La values, after four or five experiments, are associated with the initial concentration, these findings indicate they will be erroneously high when compared with an initial test K_La when no foam or surfactant deterioration had occured. It appears solutions with high initial surfactant concentrations (100 mg/L) produce greater K_La increases than at the lower surfactant concentration (50 mg/L) because higher surfactant concentration cause greater foam production.

British surfactant-enhanced aeration tests have also encountered foaming problems (Burgess and Wood, 1959; Downing, et al. 1960) even though a concentration
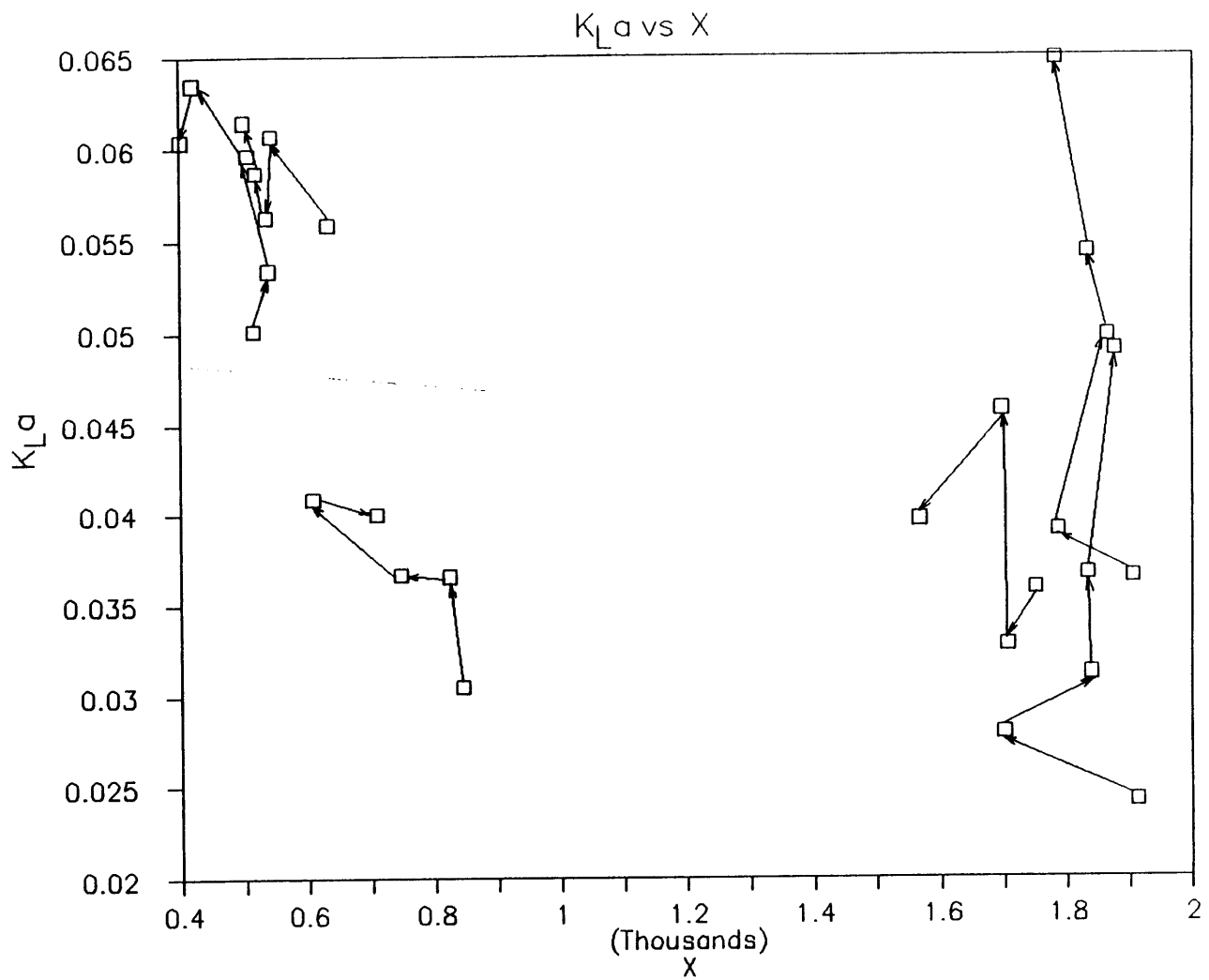
Figure 13: Effect of Repeated Aeration Runs

of only 5 mg/L was used. This suggests the aeration water be changed after every test, which for full-scale testing, is impractical. It may be better to select surfactants which produce less foam, such as Tergitol, whose foam production is much lower than DSS at the same concentration and gas flow rate.

An antifoaming agent was used to assess its effects on X and $K_L a$ (Figure 14). Two or three aeration tests on a surfactant solution produced a dense and compact foam. These tests also verified the increase in $K_L a$ and a decrease in X with repeated testing. An addition of 1 ml of an antifoaming agent was sufficient to dissipate the foam, leaving the aeration surface completely foam-free. An immediate reduction in $K_L a$ was observed in every case but one, after the addition of the antifoaming agent and the X value remained the same before and after the addition of the antifoam agent. In the lower surfactant concentration (X < 1000), a slight decrease in X values from the initial value was observed, but a slight increase in X was noted using the higher concentration (X > 1000). This contradictory trend suggests two different mechanisms are at work. The decreasing X values imply less surfactants are available for surface adsorption, indicating surfactant deterioration. At the higher concentration, there is enough surfactant to overcome the loss due to deterioration and X increases because the dissipated foam releases surfactants back into the test solution. Future experimentation is necessary to confirm these preliminary results.

Again, the significant drop in $K_L a$ after the addition of antifoam agents requires careful use of these agents when reaeration tests are performed. The agent cannot be applied indiscriminately (in volume or location) without first assessing its effects on $K_L a$.

$K_La(20)$ vs. X

filled symbols: before antifoam agent
open symbols: after antifoam agent
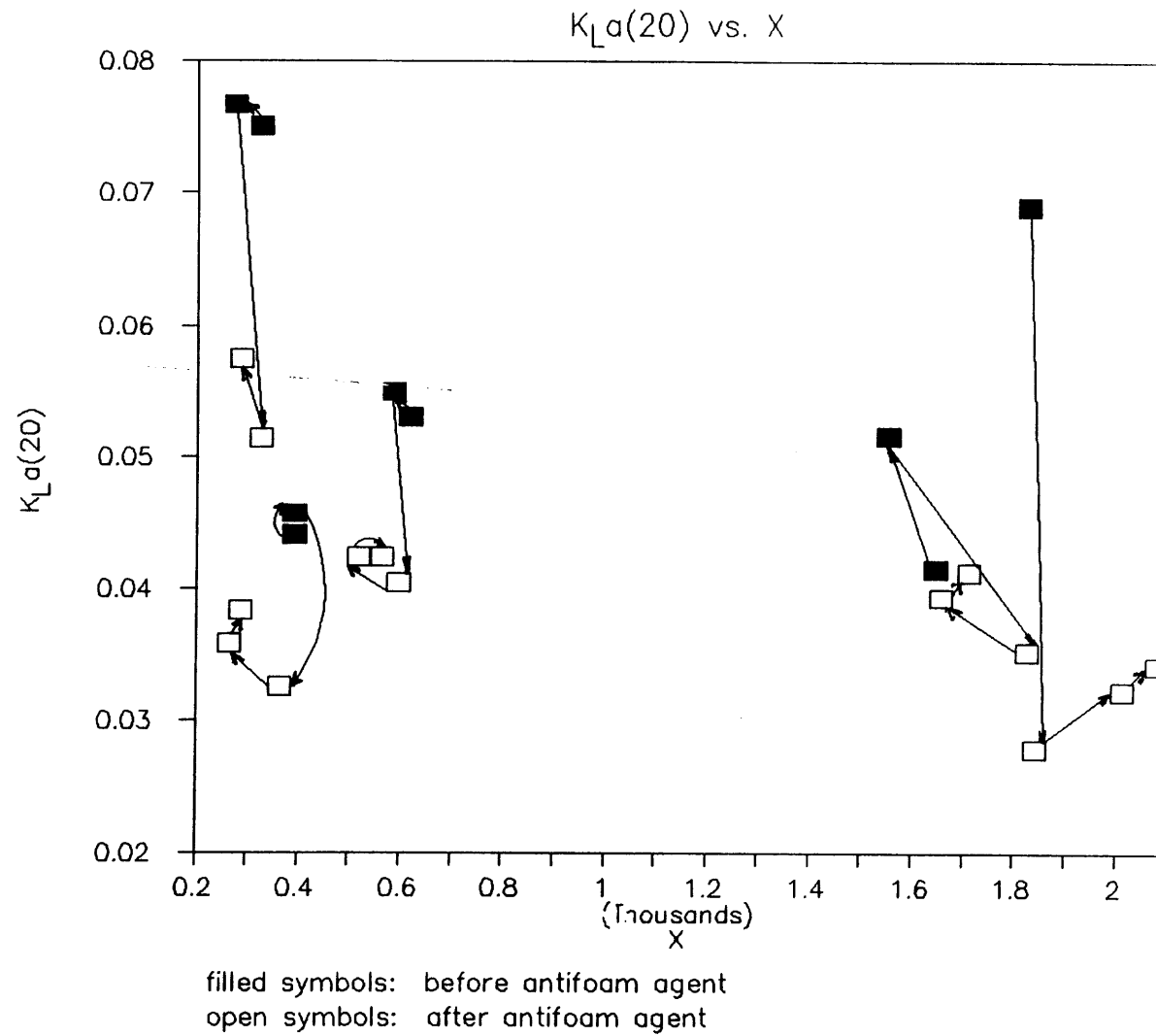
Figure 14:   Effects of Antifoaming Agent

4.3 Aeration Results

An important aspect of the significance of the DST measurement as an indicator of oxygenation capacity of process water has been to correlate the volumetric mass transfer coefficient, $K_L a$, with DST and other measurable parameters. The following experimental conditions were used in assessing these relationships:

aeration flow rate: 8, 12 and 20 L/min

surfactant concentation: 50 and 100 mg/L

surfactant type: DSS and Tergitol

In view of the results of the previous sections regarding repeated experiments and foaming problems, the following data was collected on surfactant solutions aerated at most 3 times and $K_L a$ is actually $K_L a(20°)$, using $\theta = 1.024$.

4.3.1 Bubble Sizes

Bubble sizes were determined for the surfactant solutions and tap water so the mass transfer liquid film coefficient, K_L, could be calculated from the aeration data. Averaged bubble diameters as a function of flow rate are depicted in Figure 15. The DSS solutions have larger bubbles than Tergitol solutions and, in general for both surfactants, the higher concentration solutions have smaller bubbles at each flow rate. These observations are consistent with the higher surface tension solutions having larger bubbles because of the higher shear forces necessary to detach bubbles. The large bubble size at 20 L/min for 51.5 mg/L DSS can be explained by bubble coalescence at the high exit velocity at the diffuser stone. This phenomenon was not observed with the Tergitol solution.
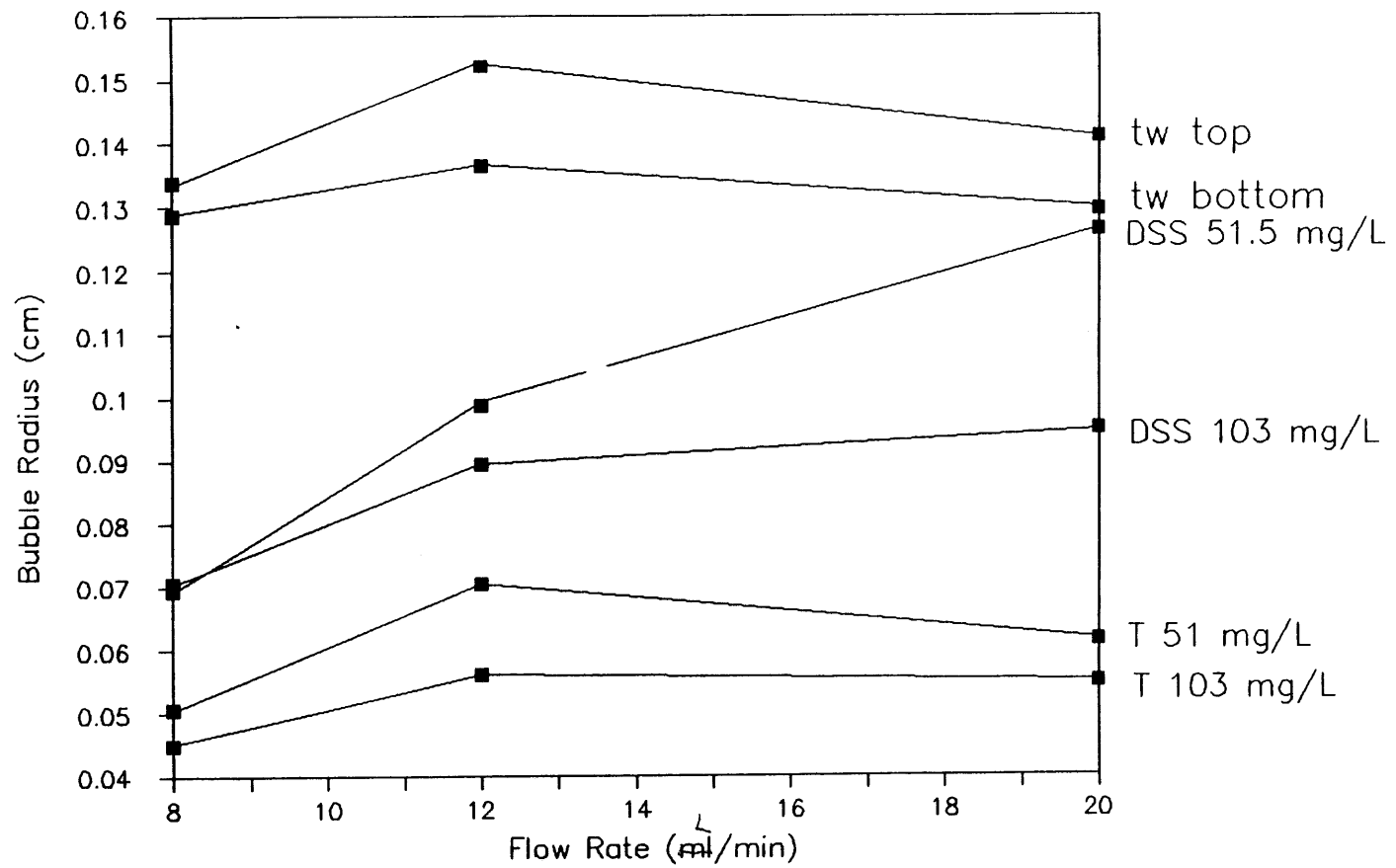
Figure 15: Bubble Radius vs. Flow Rate

An interesting aspect in Figure 15 is the relationship between bubble sizes from measurements taken at the top and at the bottom of the aeration tank for tap water. The consistently larger bubbles at the top as compared with the bubbles at the bottom show the bubbles expand, even in this short aeration column, as they rise because of the reduction in hydrostatic pressure. A quick calculation shows increase in size from the hydrostatic pressure reduction over-compensates any loss in size due to oxygen transfer.

4.3.2 K_La and DST Parameters

The first result demonstrates the relationship between K_La and X, the slope of the DST function for each aeration experiment. These results are shown in Figure 16 for Tergitol solutions and Figure 17 for DSS solutions. They show, as expected, as air flow rates increased, K_La increased for the same surfactant concentration. A more defined K_La range is observed at each flow rate for Tergitol solutions than for DSS solutions. This may result from less foaming of the Tergitol solutions so more consistent data were collected for each experiment.

For surfactant solutions, there exists a clearly defined range of X values for each concentration. For both surfactants at 50 mg/L, $600 \leq X \leq 1000$; at 100 mg/L, Tergitol solutions showed $1550 \leq X \leq 2100$, and for DSS solutions, $1900 \leq X \leq 2000$. This again confirms the correlation of high X values with high surfactant concentrations. These results are not the same as in the previous section discussing the model fit. Those surfactant solutions were not aerated and this difference contributes to the large X range for each concentration in the aerated solution. Aeration causes greater interface turbulence and surfactant concentrations may not be consistent throughout the tank. The grab samples would tend to have a
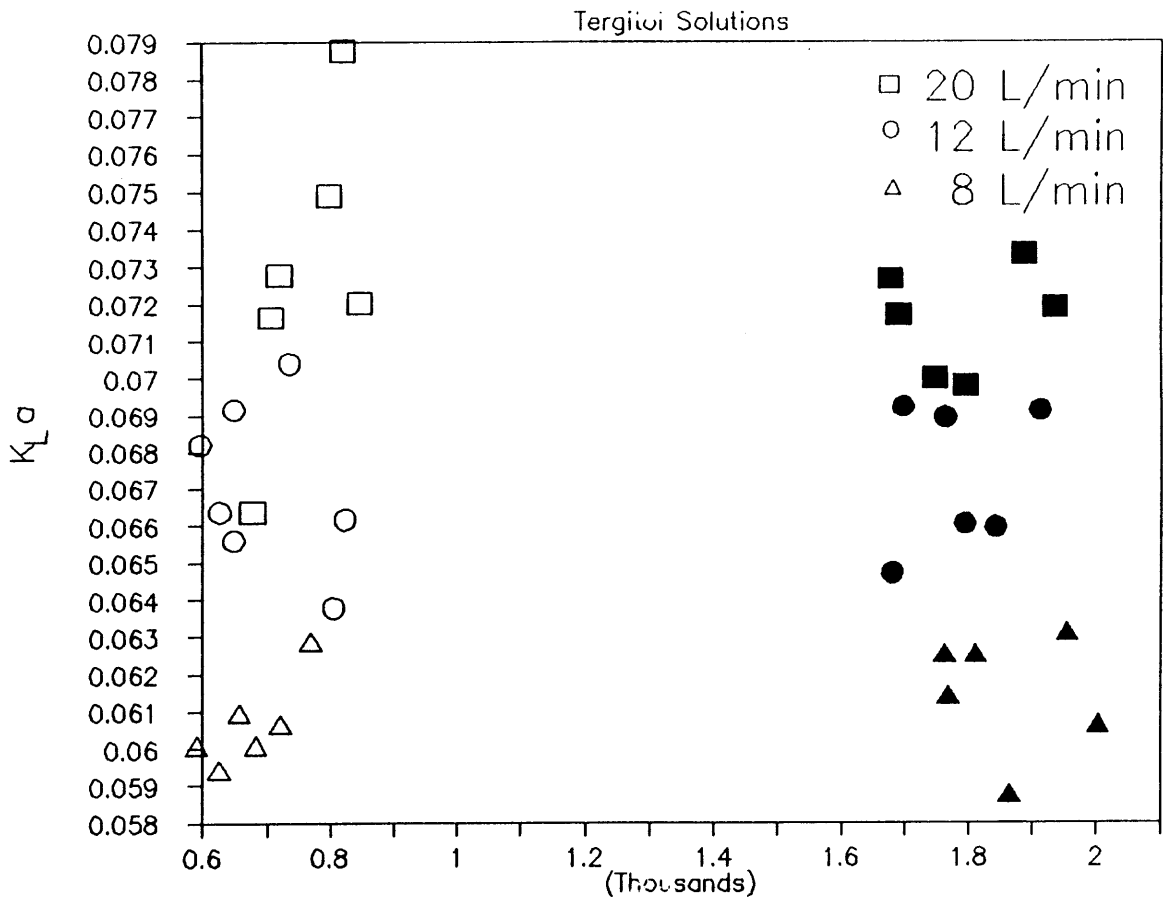
Figure 16: $K_L a$ vs. X for Tergitol Solutions
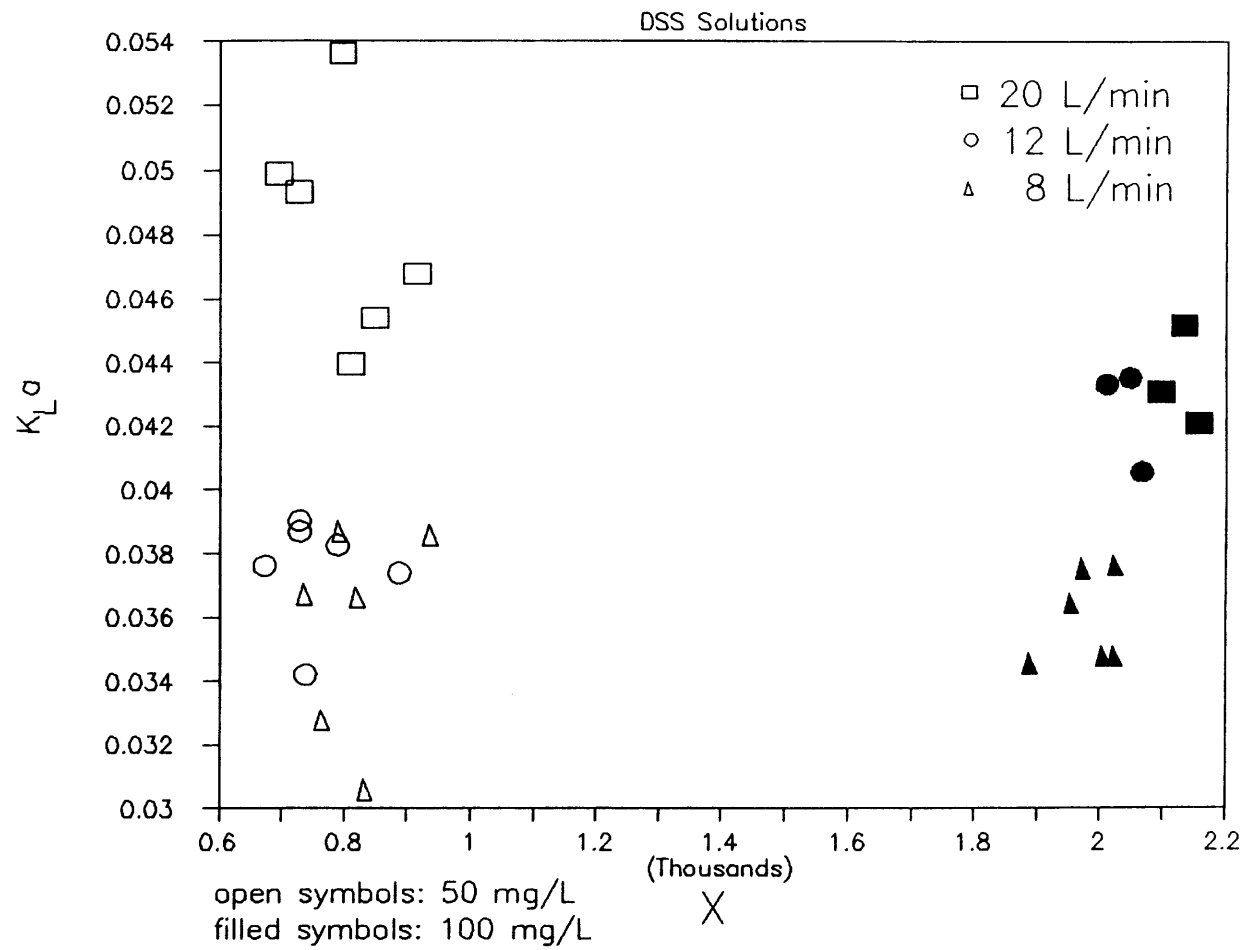
Figure 17: $K_L a$ vs. X for DSS Solutions

wider range of X for each concentration and flow rate. This phenomenon; however, needs to be investigated more fully by increasing the number of concentrations and perhaps more careful attention to aeration techniques.

A close examination of the $K_L a$ range between DSS and Tergitol solutions, at the same concentration and flow rate, reveal $K_L a$ for DSS solutions to be much lower than for the Tergitol solutions. This implies DSS is better at inhibiting oxygen transfer, either by decreasing the available surface area for transfer, A, or by decreasing K_L. Figure 15 shows DSS has larger bubbles than Tergitol at the same flow rate, indicating A is reduced in DSS solutions.

From the above discussion, the X parameter alone provides insufficient information to adequately predict $K_L a$. X qualifies the aeration potential (high X implies low aeration) but does not quantify the aeration capacity. The second result demonstrates the relationship between $K_L a$ and DST, aeration flow rate ("flow") and duNouy. The DST measurement was calculated using:

$$\text{DST} = \gamma_\infty + \frac{X}{C_o \sqrt{t_r}} \qquad (25)$$

where:

t_r = bubble retention time in aeration tank;

γ_∞ = intercept of linear model (Equation 23);

X = slope of linear model (Equation 23).

for each aeration sample. The model fitting the parameters is:

$$K_L a = 0.01732 + 0.0009144(\text{flow}) - 0.001086(\text{DST}) + 0.001809(\text{duNouy}) \qquad (26)$$

with an R^2 of 0.904. Table 10 lists the pertinent statistical information and Figure 18 shows the relationship between the predicted and actual $K_L a$. This correlation shows $K_L a$ is well-predicted by the chosen parameters.

81
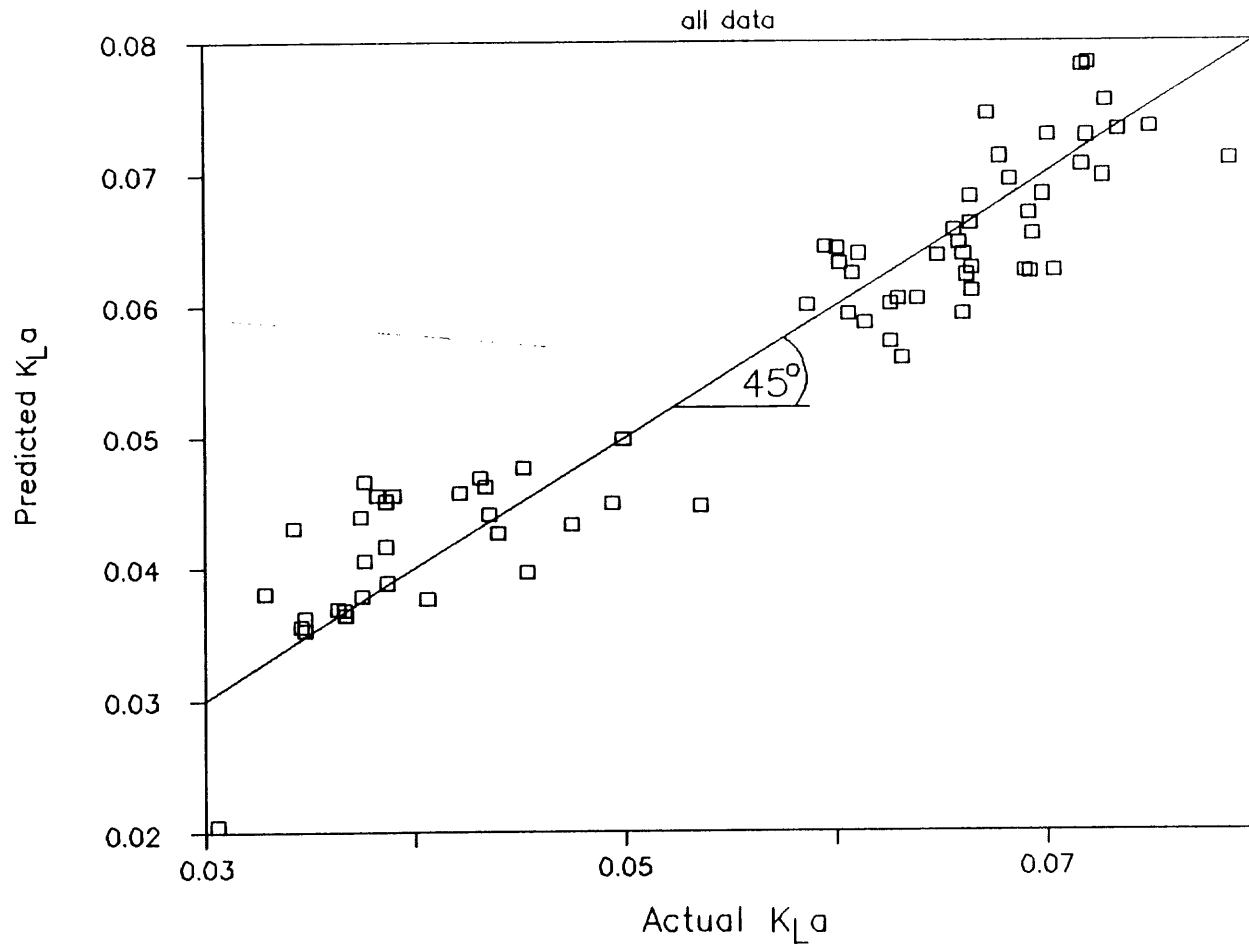
Figure 18: Predicted K_La vs. Actual K_La

variable	parameter estimate	standard error	t for H_o	prob $\geq$ t
intercept	0.01732	0.011925	1.452	0.1511
flow	0.0009144	0.0001068	8.56	0.0001
DST	-0.001086	0.0001863	-5.832	0.0001
duNouy	0.001889	0.00008122	23.26	0.0001

Table 10: K_La as a Function of DST, DuNouy and Flow

4.3.3 K_L vs. DST

The opaque aeration vessel used for K_La determinations prohibited the simultaneous determination of bubble radii during the unsteady-state aeration tests. In order to determine size, bubbles were photographed in a clear acrylic column, different in geometry and size than the aeration vessel. This modification in experiment technique required that X, γ_∞, and K_La were averaged for each air flow rate and surfactant concentration; therefore, K_L's were calculated using the average bubble radii. This data reduction was used because no other practical alternative was available.

The bubble size and terminal rise velocity were used to calculate retention times (see Sections 3.6 and 3.7). For the 20 L/min flow rate, faster water counter currents (downward) generated at the diffuser, and turbulent surface conditions entrained the bubbles forcing them downward and lengthening their retention times; therefore, the calculated retention times were doubled. With longer retention times, the surface area ages with more surfactants adsorbing at the interface producing a hydrolayer. Surface renewal is retarded and K_L decreases. Whereas faster water currents generated by the diffuser implies the bubble retention times should be shorter, the counter current of the short aeration column entrained bubbles. This
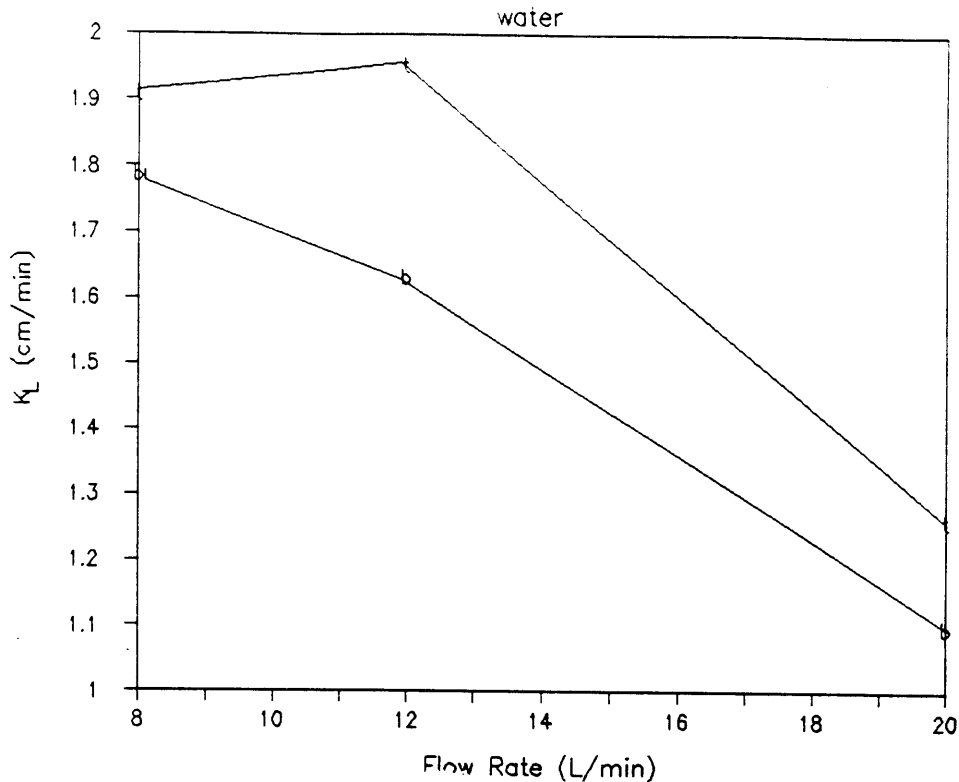
Figure 19: K_L vs. Flow Rate

was observed more emphatically at the 20 L/min air flow rate than at any other flow rate. The low K_L values of tap water confirms this decrease (Figure 19). Although K_L is reduced at 20 L/min, $K_L a$ is high; the large increase in transfer area more than compensates for the decrease in K_L.

Although the DSS data in Figure 20 is similar to the Tergitol data, there is one difference in the value of bubble radius used in the 50 mg/L DSS solution at 20 L/min. In Figure 15 the radius is much larger than would be expected based on the radii of the other sets of data. If bubble radius were changed to 0.1 cm, then DST would equal 67 dyne/cm, $K_L would be 0.2846$ cm/min and retention time is approximately 2.89 sec. This correction is applied to that data point.

The Tergitol data in Figure 20 are represented by the filled symbols and the DSS data by open symbols. Both lie in relatively straight lines as a function of

concentration. The high surfactant concentration has lower DST values than the lower surfactant concentration, at each flow rate, as expected from previous discussions. The K_L values at each flow rate for the high surfactant concentration are also lower than K_L for the lower surfactant concentration as previously observed since more surfactants have an opportunity to adsorb onto the interface and reduce K_L.

Note the highest DST value corresponds to the highest K_L value. High DST values imply that less surfactants adsorb at the interface to inhibit mass transfer; therefore, K_L should be higher. The opposite is observed at the low DST and correspondingly low K_L readings. From the linearity of the lines and the similarity of the slope, it appears K_L can be predicted for these conditions with these surfactants.

open symbols: DSS solutions
closed symbols: Tergitol solutions
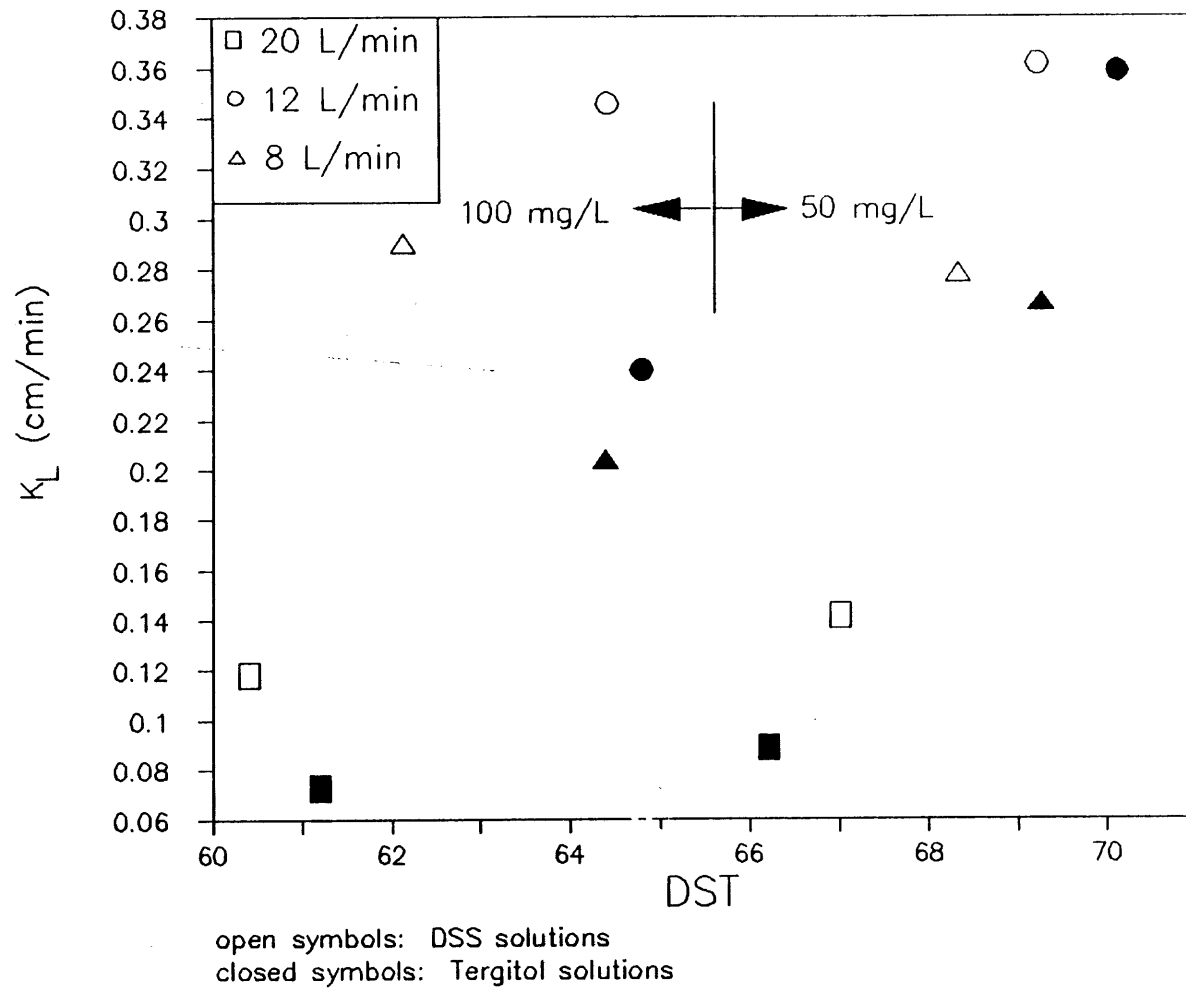
Figure 20: K_L vs. DST

Chapter 5

Conclusions

This dissertation correlates the volumetric mass transfer coefficient, $K_L a$, and the liquid film coefficient, K_L, with dynamic surface tension (DST) measurements. This new water quality indicator, along with other easily measured aeration parameters, allows for the rapid estimation of $K_L a$ and K_L. The DST measurements are an attempt to estimate $K_L a$ and K_L in the presence of surface active agents and may also facilitate using surface renewal theory in describing K_L.

This work began with a search for DST measuring techniques suitable for lab research. Of the various DST measuring techniques available, the maximum bubble pressure method was selected on the basis of its design and cost. The DST measuring device constructed in the lab was able to give accurate, reproducible results when daily fluctuations in experimental conditions were compensated. At this time the friction factor was an appropriate correction to the data.

The mathematical model developed describes the DST versus bubble life relationship. Statistical analysis of several data sets showed acceptable model fit. The model requires the initial surfactant concentration; since this concentration

is not readily known under normal process conditions, it must be estimated or correlated in some way. Another mathematical model, not relying on the initial concentration, was formulated but judged unacceptable because of a lack of fit.

The slope parameter, X, correlated to surfactant concentrations. High X values corresponded to high surfactant concentration. The intercept parameter, γ_∞, correlated to the equilibrium static surface tension measurement as measured by the du Nouy ring tensiometer. The correlations of γ_∞ versus duNouy and X versus duNouy were acceptable.

The aeration tests showed $K_L a$ was reduced in the presence of surfactants with larger decreases in $K_L a$ occurring with higher surfactant concentrations. The aeration tests also confirmed high X values corresponded to higher surfactant concentrations. The X value in aerated solutions had a larger variance than the X values in non-aerated solutions, and suggested turbulence may cause surfactant gradients to exist. A linear model relating $K_L a$ to DST, aeration flow rate and the du Nouy measurement was formulated and had a high degree of fit ($R^2 = 0.904$).

Repeated unsteady state surfactant aeration testing showed $K_L a$ increased as the number of experiments on the sample solution increased. In general, X decreased with each experiment, suggesting surfactants deteriorated or were lost from the system. After a few aeration experiments on a surfactant solution, the foam changed from light and airy to dense and compact. Fresh surfactant solutions should be used during unsteady-state testing.

The effect of an antifoaming agent was tested on these solutions. A small quantity of antifoam agent added to the solution dissipated the foam and produced a significant drop in $K_L a$. This result stresses the need for careful application of antifoam during unsteady-state testing and process operations.

Suitable averaging on aeration data, coupled with bubble sizes, were used to calculate K_L. High DST values, indicating surfactant adsorption was not complete, were associated with high K_L values. Furthermore, K_L can be estimated by aeration flow rate, surfactant concentration and DST value.

This dissertation showed the DST measurement can be an effective and useful water quality indicator. A high DST or low X value indicates surfactant adsorption is low and mass transfer coefficients are high. K_L and K_La can be estimated from aeration parameters, surfactant concentration and the DST value. In particular, DST measurements eliminate the need for process water testing to calculate K_La, and provides information regarding the water quality. Although more testing and further research are required to strengthen the correlations, the DST parameter has the potential of becoming a major water quality indicator.

Chapter 6

Future Work

This work demonstrated the usefulness of the DST measurement as a water quality indicator and in predicting $K_L a$. Further research; however, is necessary to improve data acquisition and develop more robust correlations with K_L. The following are suggestions for future research areas.

1. Friction factor correction. From observations of barometric pressure fluctuations and their magnitude in relation to bubble formation pressure, it is suggested these fluctuations be recorded simultaneously and used to reconcile the data. The friction factor may have an different formulation.

2. Model fit. Equation 23 adequately models the observed data; however, since initial surfactant concentration is not readily available for process water conditions, a new model which does not use this concentration, is required.

3. Aeration tests. Additional aeration tests should be performed on different surfactants to confirm and broaden these findings. In particular, a wider range of surfactant concentrations should be studied as well as a greater

number of flow rates. In addition, bubble sizes must be determined in the aeration tank simultaneously with the DST measurement and $K_L a$.

4. Process water conditions. DST measurement and aeration tests must be performed on process water in order to verify the theory and the correlations.

References

ASCE Oxygen Transfer Standards Committee (1984), "A Standard for the Measurement of Oxygen Transfer in Clean Water", July 1984.

Austin, M., Bright, B.B. and Simpson, E.A. (1967), "The Measurement of the Dynamic Surface Tension of Manoxol OT Solutions for Freshly Formed Surfaces", *J. Colloid and Interface Sci.*, 23, 108-112.

Barnhart, E.L. (1969), "Transfer of Oxygen in Aqueous Solutions", *J. Sanit. Engr. Div.*, ASCE, 95, 645-661.

Bendure, R.L. (1971), "Dynamic Surface Tension Determination with the Maximum Bubble Pressure Method", *J. Colloid and Interface Sci.*, 35, 239-248.

Bewtra, J.K. and Nicholas, W.R. (1964), "Oxygen from Diffused Air in Aeration Tanks", *J. Wat. Pollut. Control Fed.*, 36, 1195-1223.

Bikerman, J.J. (1973), *Foams*, Springer-Verlag, New York.

Bohr, N. (1909), "Determination of the Surface Tension of Water by the Method of Jet Vibration", *Roy. Soc. London, Phil. Trans., Ser. A.*, 209, 281-317.

Burcik, E.J. (1950), "The Rate of Surface Tension Lowering and Its Role in Foaming", *J. Colloid Sci.*, 5, 421-436.

Burgess, S.G. and Wood, L.B. (1959), "Some Experiments in Aeration", *J. Inst. Sewage Purif.*, 258-270.

Carver, C.E., Jr. (1956), "Absorption of Oxygen in Bubble Aeration", in *Biological Treatment of Sewage and Industrial Wastes, Vol. 1*, (edited by McCabe, J. and Eckenfelder, W.W., Jr.), Reinhold Pub. Co., New York, pp. 149-171.

92

Caskey, J.A. and Barlage, W.B., Jr. (1971), "An Improved Experimental Technique for Determining Dynamic Surface Tension of Water and Surfactant Solutions", *J. Colloid and Interface Sci.*, 35, 46-52.

Chistyakov, B.E., Balakhonov, G.G., Bukhshtab, Z.I., Polkovnichenko, I.T. and Shapovalova, T.V. (1979), "Foaming of Aqueous Solutions of Triethanolamine Salts of Alkyl Phosphates", *J. Appl. Chem. (USSR)*, 52, 1560-1561.

Dankwerts, P.V. (1951), "Significance of the Liquid-Film Coefficient in Gas Adsorption", *Ind. Engr. Chem.*, 43, 1460-1467.

Davis, J.T. and Rideal, E.K. (1961), *Interfacial Phenomena*, 2nd Ed., Academic Press.

Defay, R. and Hommelen, J.R. (1958), "I. Measurement of Dynamic Surface Tension of Aqueous Solutions by the Oscillating Jet Method", *J. Colloid and Interface Sci.*, 13, 553-564.

Defay, R. and Hommelen, J.R. (1959), "III. The Importance of Diffusion in the Adsorption Process of Some Alcohols and Acids in Dilute Aqueous Sollutions", *J. Colloid Sci.*, 14, 411-418.

Detwiler, A. (1979), "Surface Active Contamination on Air Bubbles in Water", In *Surface Contamination, Genesis, Detection and Control*, Vol. 2, (edited by K.L. Mittal), Plenum Press, New York, 993-1007.

Downing, A.L., Bayley, R.W. and Boon, A.G. (1960), "The Performance of Mechanical Aerators", *J. Inst. Sewage Purif.*, 231-242.

du Nouy, P. Lecomte (1918-1919), "A New Apparatus for Measuring Surface Tension", *J. Gen. Physio.*, 1, 521-524.

Eckenfelder, W.W., Jr. and Ford, D.L. (1968), "New Concepts in Oxygen Transfer and Aeration", In *Advances in Water Quality Improvement*, (edited by Gloyna, E.F. and Eckenfelder, W.W. Jr.), University of Texas Press, 215-236.

Eckenfelder, W.W., Jr., Raymond, L.W. and Lauria, D.T. (1956), "Effect of Various Organic Substances on Oxygen Adsorption Efficiency", *Sewage Ind. Wastes J.*, 28, 1357-1364.

Ewing, L., Redmon, D.T. and Wren, J.D. (1979), "Testing and Data Analysis of Diffused Aeration Equipment", *J. Wat. Pollut. Control Fed.*, 51, 2384-2401.

Freud, B.B. and Freud, H.Z. (1930), "A Theory of the Ring Method for the Determination of Surface Tension", *Amer. Chem. Soc. J.*, 52, 1772-1782.

Gilanyi, T., Stergiopoulos, Chr. and Wolfram, E. (1976), "Equilibrium Surface Tension of Aqueous Surfactant Solutions", *Colloid Poly. Sci.*, 254, 1018-1023.

Haberman, W.L. and Morton, R.K. (1953), "An Experimental Investigation of the Drag and Shape of Air Bubbles Rising in Various Liquids", Navy Department, David W. Taylor Model Basin Report 802, 47 p.

Harkins, W.D. (1952), *The Physical Chemistry of Surface Films*, Reinhold Press, New York.

Harkins, W.D. and Jordon, H.J. (1930), "A Method for the Determination of Surface and Interfacial Tension from the Maximum Pull on a Ring", *Amer.*

Chem. Soc. J., 32, 1751-1772.

Higbie, R. (1935), "The Rate of Absorption of a Pure Gas into a Still Liquid During Short Periods of Exposure", *AIChE Trans.*, 31, 365-388.

Hommelen, J.R. (1959), "The Elimination of Errors Due to Evaporation of the Solute in the Determination of Surface Tension", *J. Colloid Sci.*, 14, 385-400.

Huh, C. and Mason, S.G. (1975), "A Rigorous Theory of Ring Tensiometry", *Colloid Poly. Sci.*, 253, 566-580.

Hunter, J.S., III (1979), "Accounting for the Effects of Water Temperature in Aeration Tests," in Proceedings Toward an Oxygne Transfer Standard, EPA 600/9-78/021, 85-89.

Hwang, H.J. and Stenstrom, M.K. (1979), "The Effect of Surface Active Agents on Oxygen Transfer", Water Resources Program Report 79-2, UCLA School of Engineering and Applied Science, pp. 58.

Ippen, A.T. and Carver, C.E., Jr. (1954), "Basic Factors of Oxygen Transfer in Aeration Systems", *Sewage Works J.*, 26, 813-827.

Jobert, P.P. and Leblond, J. (1979), "Effects of Surface Active Materials on the Hydrodynamic Development in a Liquid Jet", *J. Colloid and Interface Sci.*, 68, 478-485.

Jones, T.G., Durham, K., Evans, W.P. and Camp, M. (1957), "The Stability of Foams", in *Gas/Liquid and Liquid/Liquid Interfaces*, Proceedings of the 2nd International Congress on Surface Activity, Academic Press, NY, 225-230.

Joos, P. and Rillaerts, E. (1981), "Theory on the Determination of the Dynamic Surface Tension with the Drop Volume and Maximum Bubble Pressure Method, *J. Colloid and Interface Sci.*, 79, 96-100.

Joos, P. and Ruyssen, R. (1967), "The Foaming Properites of Saponins: Time and Electrolytes Effects", in *Chemistry, Physics and Application of Surface Active Agents*, Proceedings of the IVth International Congress of Surface Active Substances, Brussels, (edited by Overbeek, J.Th.G.), Gordon Breach Sci. Pub., New York, pp. 1143-1151.

Kloubek, J. (1972), "Measurement of the Dynamic Surface Tension by the Maximum Bubble Pressure Method. III. Factors Influencing the Measurement a High Frequency of Bubble Formation and an Extension of Zero Age of Surface", *J. Colloid and Interface Sci.*, 41, 7-16.

Kloubek, J. (1972), "Measurement of the Dynamic Surface Tension by the Maximum Bubble Pressure Method. IV. Surface Tension ofAqueous Solutions of Sodium Dodecyl Sulfate", *J. Colloid and Interface Sci.*, 41, 17-32.

Kochurova, N.N., Shvchenkov, Yu.A. and Rusanov, A.I. (1974), "Determination of Surface Tension of Water by the Method of an Oscillating Jet", *Colloid J. of the USSR*, 36, 725-727.

Lange, H. (1965), "Dynamic Surface Tension of Detergent Solutions at Constant and Variable Surface Area", *J. Colloid Sci.*, 20, 50-61.

Lauwers, A.R. and Ruyssen, R. (1967), "Foaming Properties of Macro-molecular Surface Active Agents - β Lactoglobin", In *Chemistry, Physics, and Application of Surface Active Agents*, (edited by Overbeek, J.Th.G.), Gordon and

Breach Science Pub., New York, 1153-1159.

Lewis, A.R. and Whitman, W.G. (1924), "Principles of Gas Absorption", *Ind. Engr. Chem*, 16, 1215-1220.

Lister, A.R. and Boon, A.G. (1973), "Aeration in Deep Tanks: An Evaluation of a Fine Bubble Diffuser-Air System", *Inst. Sew. Purif.*, 3-18.

Lukenheimer, K. and Wante, K.D. (1981), "Determination of the Surface Tension of Surfactant Solutions Applying the Method of Lecomte du Nouy (Ring Tensiometer)", *Colloid Poly. Sci.*, 259, 354-366.

Lynch, W.O. and Sawyer, C.N. (1954), "Physical Behavior of Synthetic Detergents I. Preliminary Studies on Frothing and Oxygen Transfer", *Sewage Indust. Wastes*, 26, 1193-1201.

Lynch, W.O. and Sawyer, C.N. (1960), "Effects of Detergents on Oxygen Transfer in Bubble Aeration", *J. Wat. Pollut. Control Fed.*, 32, 25-40.

Mancy, K.H. and Okun, D.A. (1960), "Effects of Surface Active Agents on Bubble Aeration", *J. Wat. Pollut. Control Fed.*, 32, 351-364.

Mancy, K.H. and Okun, D.A. (1965), "The Effects of Surface Active Agents on Aeration", *J. Wat. Pollut. Control Fed.*, 37, 212-227.

Mancy, K.H. and Barlage, W.E., Jr. (1968), "Mechanism of Interference of Surface Active Agents with Gas Transfer in Aeration Systems" in *Advances in Water Quality*, (edited by Gloyna, F. and Eckenfelder, W.W., Jr.), University of Texas Press, pp. 262-286.

Metcalf and Eddy, Inc. (1979), *Wastewater Engineering: Treatment, Disposal, Reuse*, 2nd edition, McGraw-Hill Book Co., New York, pp 203.

Motarjemi, M. and Jameson, G.T. (1978), "Effect of Bubble Size on Oxygen Utilization in Aeration Processes", In *New Processes of Waste Water Treatment and Recovery*, (edited by Mattock, G.), Ellis Horwood, Ltd., Sussex, England, 48-57.

Otoski, R.A., Brown, L.C. and Gilbert, R.G. (1979), "Bench and Full-scale Tests for Alpha and Beta Coefficient Variability Determination", *Proc. Purdue Ind. Waste Conf.*, 835-852.

Pasveer, A. (1955), "Research on Activated Sludge. VI. Oxygenation of Water with Air Bubbles", *Sewage Ind. Wastes J.*, 27, 1130-1146.

Pierson, F.W. and Whitaker, S. (1976), "Studies of the Drop-weight Method for Surfactant Solutions. II. Experimental Results for Water and Surfactant Solutions", *J. Colloid and Interface Sci.*, 54, 219-230.

Rosen, M.J. (1978), *Surfactants and Interfacial Phenomena*, John Wiley and Sons, New York.

Schmit, F.L., Wren, J.D. and Redmon, D.T. (1978), "The Effect of Tank Dimensions and Diffuser Placement on Oxygen Transfer", *J. Wat. Pollut. Control Fed.*, 50, 1750-1767.

Shah, D.O., Djabbarah, N.J. and Wasan, D.T. (1978), "A Correlation of Foam Stability with Shear Surface Viscosity and Area per Molecule in Mixed Surfactant Systems", *Colloid Poly. Sci.*, 256, 1002-1008.

Stenstrom, M.K. and Gilbert, R.G. (1981), "Effects of Alpha, Beta, and Theta Factors Upon the Design, Specification, and Operation of Aeration Systems", *Wat. Res.*, 15, 643-654.

Stenstrom, M.K., Brown, L.C. and Hwang, H.J. (1981) "Oxygen Transfer Parameter Estimation", *J. Envir. Engr. Div. ASCE*, 379-397.

Sugden, S. (1922), "Determination of Surface Tension from the Maximum Pressure in Bubbles", *J. Chem. Soc.*, 121, 858-866.

Sugden, S. (1924), "The Determination of Surface Tension from the Maximum Pressure in Bubbles, Part II", *J. Chem. Soc.*, 125 27-31.

Suzuki M., Okazaki, S., Moriwaki, T. and Sugimitsu, H. (1972), "Measurements of Dynamic Surface Tension of a Detergent Solution", In *Proceedings of the International Congress on Surface Active Substances, 6th.*, Zurich, 881-888.

Thomas, W.D.E. and Potter, L. (1975), "I. An Oscillating Jet Relative Method for Determining Dynamic Surface Tension", *J. Colloid and Interface Sci.*, 50, 397-412.

Thomas, W.D.E. and Hall, D.J. (1975) "II. Adsorption of Surfactants in Dilute Aqueous Solutions. Anomalous Oscillating Jet Phenomena", *J. Colloid and Interface Sci.*, 51, 328-334.

Vijayan, S. and Ponter, A.B. (1972), "Dynamic Surface Tension Studies Using an Oscillating Jet", *Indian Chem. Engr. XIV*, 26-32.

Yoshida, F. and Akita, K. (1965), "Performance of Gas Bubble Columns: Volumetric Liquid-Phase Mass Transfer Coefficient and Gas Hold-up", *AIChE*

J., 11, 9-13.

100

Appendix A

All First Day Data

All First Day Data

run	conc (mg/l)	kla (1/min)	dunouy (dyn/cm)	flow (1/min)	inter (dyn/cm)	slope	id
64	51.5	0.062925	59.82	8	64.0962	780.96	111
65	51.5	0.060101	60.32	8	63.0543	691.44	111
66	51.5	0.059996	60.68	8	63.4614	603.13	111
72	51.5	0.060715	60.35	8	63.4566	733.72	111
73	51.5	0.061009	60.51	8	62.9832	665.80	111
74	51.5	0.059447	60.45	8	62.6752	638.22	111
60	51.5	0.063785	58.31	12	63.4772	815.82	112
61	51.5	0.065571	60.09	12	63.2660	652.79	112
62	51.5	0.066353	61.15	12	64.8186	635.68	112
68	51.5	0.070340	58.24	12	61.9228	745.87	112
69	51.5	0.069097	60.48	12	62.6879	658.49	112
70	51.5	0.068197	61.64	12	62.9905	601.25	112
96	51.5	0.066175	58.93	12	62.5213	831.17	112
97	51.5	0.066406	58.17	12	63.7553	694.53	112
98	51.5	0.066393	58.73	12	63.2596	680.20	112
56	51.5	0.067153	59.19	20	59.6868	791.09	113
57	51.5	0.071968	60.68	20	57.8398	854.43	113
58	51.5	0.071666	60.83	20	59.7225	716.23	113
76	51.5	0.065797	55.31	20	61.0993	833.36	113
77	51.5	0.066329	57.48	20	62.4827	759.27	113
78	51.5	0.067694	59.33	20	63.7718	676.97	113
0	51.5	0.078715	58.90	20	61.7203	828.12	113
1	51.5	0.074894	60.09	20	61.8686	804.54	113
2	51.5	0.072802	60.51	20	61.4901	728.39	113
80	103	0.063050	53.94	8	56.7889	1960.94	121
81	100	0.060554	56.11	8	56.9481	2015.08	121
82	100	0.058648	56.50	8	57.6440	1874.08	121
92	100	0.062513	54.34	8	56.7106	1814.60	121
93	100	0.061320	55.15	8	56.9217	1775.02	121
94	100	0.062524	56.14	8	57.3352	1773.46	121
48	103	0.069170	55.32	12	55.8544	1917.52	122
49	100	0.066008	56.11	12	56.2908	1797.15	122
50	100	0.069269	57.06	12	56.9579	1702.41	122
84	100	0.065969	54.01	12	56.4839	1857.28	122
85	100	0.068942	55.45	12	56.4060	1773.87	122
86	100	0.064747	56.40	12	57.3913	1689.35	122
44	103	0.069779	54.21	20	55.8746	1803.83	123
45	100	0.072663	55.09	20	56.4948	1681.85	123
46	100	0.071675	55.94	20	57.2012	1693.20	123
88	100	0.073373	56.07	20	54.0652	1895.19	123
89	100	0.071870	55.94	20	54.0183	1944.59	123
90	100	0.070025	56.04	20	55.0305	1754.05	123

All First Day Data

run	conc (mg/L)	kla (1/min)	dunouy (dyn/cm)	flow (L/min)	inter (dyn/cm)	slope	id
51	51	0.030491	36.18	8	58.1907	844.25	211
52	50	0.036621	45.38	8	59.2843	822.86	211
53	50	0.036694	45.19	8	60.0741	746.46	211
2	50	0.038602	49.13	8	60.0720	943.67	211
3	50	0.038688	47.38	8	61.0705	802.20	211
4	50	0.032782	47.11	8	61.6280	772.95	211
33	51	0.038178	48.38	12	59.0946	797.85	212
34	50	0.038623	48.35	12	59.9878	734.68	212
35	50	0.038918	49.26	12	61.2064	734.55	212
24	50	0.037384	48.90	12	60.1386	896.07	212
25	50	0.034174	48.18	12	61.4031	750.64	212
26	50	0.037539	49.55	12	61.2871	683.74	212
16	51	0.053532	45.12	20	59.9640	805.92	213
17	50	0.049340	45.33	20	60.9299	730.56	213
18	50	0.049833	48.27	20	61.8721	702.04	213
40	50	0.045313	43.14	20	60.3022	861.44	213
41	50	0.042877	44.62	20	60.6680	818.06	213
42	50	0.047101	44.71	20	59.1957	899.13	213
20	103	0.037586	44.68	8	52.8108	2034.12	221
21	100	0.034727	42.50	8	52.8897	2007.18	221
22	100	0.037436	44.48	8	54.9626	1982.89	221
36	100	0.034748	40.74	8	50.5400	2030.88	221
37	100	0.034529	40.94	8	51.3822	1892.98	221
38	100	0.036327	41.39	8	50.5188	1960.52	221
28	103	0.043271	45.48	12	51.5327	2017.54	222
29	100	0.040552	43.68	12	55.5769	2078.81	222
30	100	0.043459	45.22	12	52.4220	2058.42	222
32	103	0.043051	42.98	20	52.5469	2102.89	223
33	100	0.042086	42.25	20	51.6106	2163.73	223
34	100	0.045137	43.20	20	51.6769	2142.59	223
	0	0.079281		8			311
	0	0.079281		8			312
	0	0.098468		12			321
	0	0.098468		12			322
	0	0.120174		20			331
	0	0.120174		20			332

    id 100's = tergitol
    id 200's = DSS
    id 300's = water

103

All First Day Data

id	rad (cm)	vel (cm/s)	rettime (s)	area (cm**2)	klhr (cm/hr)	dst (dyn/cm)
111	0.050673	12.94	4.90726	38736.7	16.6028	70.9416
111	0.050673	12.94	4.90726	38736.7	15.8577	69.2969
111	0.050673	12.94	4.90726	38736.7	15.8300	68.9067
111	0.050673	12.94	4.90726	38736.7	16.0197	70.0809
111	0.050673	12.94	4.90726	38736.7	16.0973	68.9943
111	0.050673	12.94	4.90726	38736.7	15.6851	68.4373
112	0.070358	16.99	3.73749	31872.6	20.4541	71.6712
112	0.070358	16.99	3.73749	31872.6	21.0269	70.0193
112	0.070358	16.99	3.73749	31872.6	21.2776	71.3949
112	0.070358	16.99	3.73749	31872.6	22.5561	69.6390
112	0.070358	16.99	3.73749	31872.6	22.1576	69.5001
112	0.070358	16.99	3.73749	31872.6	21.8689	69.2106
112	0.070358	16.99	3.73749	31872.6	21.2205	71.1199
112	0.070358	16.99	3.73749	31872.6	21.2946	70.9404
112	0.070358	16.99	3.73749	31872.6	21.2905	70.2964
113	0.061468	15.26	4.1612	67697.1	10.1386	67.2170
113	0.061468	15.26	4.1612	67697.1	10.8655	66.2170
113	0.061468	15.26	4.1612	67697.1	10.8199	66.7447
113	0.061468	15.26	4.1612	67697.1	9.9338	69.2699
113	0.061468	15.26	4.1612	67697.1	10.0141	69.9269
113	0.061468	15.26	4.1612	67697.1	10.2202	70.4091
113	0.061468	15.26	4.1612	67697.1	11.8841	69.8395
113	0.061468	15.26	4.1612	67697.1	11.3073	69.7566
113	0.061468	15.26	4.1612	67697.1	10.9914	68.6315
121	0.044958	11.6	5.47414	48704.5	13.2311	64.9260
121	0.044958	11.6	5.47414	48704.5	12.7073	65.5607
121	0.044958	11.6	5.47414	48704.5	12.3074	65.6540
121	0.044958	11.6	5.47414	48704.5	13.1184	64.4663
121	0.044958	11.6	5.47414	48704.5	12.8681	64.5083
121	0.044958	11.6	5.47414	48704.5	13.1208	64.9151
122	0.056134	14.16	4.48446	47933.1	14.7490	64.6456
122	0.056134	14.16	4.48446	47933.1	14.0748	64.7773
122	0.056134	14.16	4.48446	47933.1	14.7701	64.9970
122	0.056134	14.16	4.48446	47933.1	14.0665	65.2544
122	0.056134	14.16	4.48446	47933.1	14.7004	64.7826
122	0.056134	14.16	4.48446	47933.1	13.8059	65.3688
123	0.054864	13.88	4.57493	83386.7	8.5528	64.0624
123	0.054864	13.88	4.57493	83386.7	8.9063	64.3579
123	0.054864	13.88	4.57493	83386.7	8.7852	65.1174
123	0.054864	13.88	4.57493	83386.7	8.9933	62.9257
123	0.054864	13.88	4.57493	83386.7	8.8091	63.1098
123	0.054864	13.88	4.57493	83386.7	8.5830	63.2312

All First Day Data

id	rad (cm)	vel (cm/s)	rettime (s)	area (cm**2)	klhr (cm/hr)	dst (dyn/cm)
211	0.069469	16.82	3.77527	21737.8	14.3363	66.7105
211	0.069469	16.82	3.77527	21737.8	17.2185	67.7543
211	0.069469	16.82	3.77527	21737.8	17.2528	67.7577
211	0.069469	16.82	3.77527	21737.8	18.1499	69.7855
211	0.069469	16.82	3.77527	21737.8	18.1903	69.3278
211	0.069469	16.82	3.77527	21737.8	15.4134	69.5842
212	0.098679	21.81	2.91151	17702.9	22.0419	68.2630
212	0.098679	21.81	2.91151	17702.9	22.2988	68.5991
212	0.098679	21.81	2.91151	17702.9	22.4692	69.8162
212	0.098679	21.81	2.91151	17702.9	21.5835	70.6416
212	0.098679	21.81	2.91151	17702.9	19.7302	70.2015
212	0.098679	21.81	2.91151	17702.9	21.6730	69.3013
213	0.126492	25.83	2.45838	19435.1	28.1519	70.0425
213	0.126492	25.83	2.45838	19435.1	25.9474	70.2487
213	0.126492	25.83	2.45838	19435.1	26.2067	70.8271
213	0.126492	25.83	2.45838	19435.1	23.8296	71.2905
213	0.126492	25.83	2.45838	19435.1	23.0745	71.1030
213	0.126492	25.83	2.45838	19435.1	24.9277	70.6648
221	0.070612	17.04	3.72652	21109.9	18.1979	63.0411
221	0.070612	17.04	3.72652	21109.9	16.8137	63.2873
221	0.070612	17.04	3.72652	21109.9	18.1253	65.2344
221	0.070612	17.04	3.72652	21109.9	16.8238	61.0604
221	0.070612	17.04	3.72652	21109.9	16.7178	61.1882
221	0.070612	17.04	3.72652	21109.9	17.5883	60.6747
222	0.089408	20.33	3.12346	20961	21.0992	62.6159
222	0.089408	20.33	3.12346	20961	19.7734	67.3393
222	0.089408	20.33	3.12346	20961	21.1909	64.0690
223	0.095123	21.25	2.98823	31414.4	14.0067	64.3575
223	0.095123	21.25	2.98823	31414.4	13.6927	64.1275
223	0.095123	21.25	2.98823	31414.4	14.6853	64.0715
311	0.128650	26.12	2.43109	7558.8	107.2010	
312	0.133860	26.81	2.36852	7077.7	114.4870	
321	0.136530	27.16	2.338	10275	97.9470	
322	0.152270	29.14	2.17913	8586.4	117.2100	
331	0.129790	26.28	2.41629	18616.3	65.9780	
332	0.141100	27.75	2.28829	16217.8	75.7350	

id 100's = tergitol
id 200's = DSS
id 300's = water

Appendix B

Antifoam Data Using DSS Solutions

Antifoam Solutions
DSS Solutions

run	conc (mg/l)	kla(20) (1/min)	du Nouy (dyne/cm)	flow (1/min)	X	inter
56	50	0.053231	46.39	12	625	64.3
57	50	0.054878	46.29	12	603	64.0
58	50	0.040184	43.72	12	601	63.5
59	50	0.042336	45.23	12	537	64.9
60	50	0.042188	45.09	12	571	64.6
61	50	0.044222	48.29	12	404	65.0
62	50	0.045598	47.84	12	409	65.2
63	50	0.032468	47.38	12	377	66.4
64	50	0.035535	47.42	12	275	66.8
65	50	0.038320	47.94	12	298	67.3
74	100	0.068840	40.17	12	1830	56.5
75	100	0.027988	42.21	12	1852	55.7
76	100	0.032360	43.56	12	2024	55.1
77	100	0.034140	42.91	12	2087	56.8
78	100	0.031136	42.56	20	1069	61.5
79	100	0.034632	41.60	20	1527	61.7
80	100	0.031096	39.57	20	1849	60.7
81	100	0.037569	44.06	20	1566	61.8
82	100	0.036348	38.33	20	2094	59.8
91	100	0.041420	57.93	20	1664	58.8
92	100	0.051678	45.48	20	1561	59.1
93	100	0.035421	42.31	20	1828	57.7
94	100	0.039528	42.05	20	1661	58.6
95	100	0.041371	42.21	20	1717	58.8
11	50	0.075120	57.78	20	342	67.7
12	50	0.076836	57.19	20	286	68.5
13	50	0.051401	55.03	20	333	67.7
14	50	0.057187	52.15	20	303	68.4

Appendix C

Data for Continuous Aeration Runs

Data for Continuous Aeration Runs

run	conc (mg/l)	kla(20) (1/min)	dunouy (dyne/cm)	flow (1/min)	slope (X)	inter
39	50	0.050123	48.61	8	514	64.4
40	50	0.053413	52.53	8	538	64.1
41	50	0.059659	51.08	8	506	64.8
42	50	0.063452	54.24	8	419	65.9
43	50	0.060413	53.93	8	401	65.6
44	50	0.060716	58.93	8	320	67.8
45	50	0.056060	65.84	8	356	66.1
46	50	0.058023	68.61	8	365	66.4
51	50	0.030491	36.18	8	844	58.2
52	50	0.036621	45.38	8	823	59.3
53	50	0.036694	45.19	8	746	60.1
54	50	0.040900	43.68	8	608	61.9
55	50	0.040017	46.80	8	708	61.8
69	100	0.024204	44.55	12	1911	53.9
70	100	0.027959	42.50	12	1699	55.4
71	100	0.031224	43.75	12	1837	53.2
72	100	0.036714	47.73	12	1932	54.8
73	100	0.049048	44.97	12	1876	56.1
86	100	0.036513	42.02	20	1903	48.3
87	100	0.039141	42.08	20	1784	49.0
88	100	0.049829	40.74	20	1864	49.2
89	100	0.054381	41.89	20	1832	50.3
90	100	0.064808	52.98	20	1781	52.1
96	100	0.035943	44.62	20	1749	61.4
97	100	0.032810	42.31	20	1705	60.3
98	100	0.045792	44.39	20	1696	60.6
99	100	0.039745	43.31	20	1566	60.9
6	50	0.055847	50.46	20	632	63.1
7	50	0.060664	52.64	20	542	62.8
8	50	0.056252	54.50	20	535	64.1
9	50	0.058652	54.24	20	518	64.0
10	50	0.061444	53.73	20	499	63.7

Appendix D

Non-aerated Solutions

Non-aerated Solutions

date	conc (mg/l)	sym	duNouy (dyne/cm)	X	inter
7.29	301.6	d	39.48	3836	44.25
	301.6	d	38.27	4123	42.37
	301.6	d	38.90	4008	42.37
7.3	200.3	d	40.33	3513	45.59
	200.3	d	42.19	3343	44.26
	200.3	d	40.19	3202	44.18
8.03	100.8	d	42.89	1648	51.13
	100.8	d	42.47	1967	49.51
	100.8	d	43.18	1872	49.55
8.04	53.0	d	49.16	938	57.00
	53.0	d	47.68	852	56.90
8.1	103.0	t	54.50	1598	56.46
	103.0	t	55.06	1627	54.51
	103.0	t	55.29	1697	55.33
	206.0	t	50.40	2004	51.66
	206.0	t	50.82	1974	51.70
	206.0	t	50.88	1983	51.12
8.12	51.5	t	57.75	684	62.64
	51.5	t	57.99	664	62.63
	51.5	t	58.64	658	62.22
8.13	309.0	t	48.84	2405	48.90
	309.0	t	49.03	2753	48.54
8.25	78.6	t	55.94	1306	57.28
	78.6	t	56.70	1277	57.61
	153.0	t	52.74	2045	52.55
8.26	153.0	t	51.79	1937	52.62
	74.0	d	48.06	1176	55.25
	74.0	d	46.87	1343	53.82

Appendix E

Averaged Data

Averaged Data

flow	conc	type	radius (cm)	kla (1/min)	label	X	inter	vel (cm/s)	kl (cm/min)
8	51.5	1	0.050673	0.060699	11	686	63.29	12.94	0.266924
12	51.5	1	0.070358	0.066924	11	691	63.19	16.99	0.357678
20	51.5	1	0.061468	0.070780	11	763	61.13	15.26	0.178102
8	103.0	1	0.044958	0.058677	12	1869	56.66	11.60	0.205224
12	103.0	1	0.056134	0.067351	12	1790	56.56	14.16	0.239352
20	103.0	1	0.054864	0.071564	12	1795	55.46	13.88	0.146193
8	51.0	2	0.069469	0.035460	21	822	60.05	16.82	0.277876
12	51.0	2	0.098679	0.037469	21	766	60.52	21.81	0.360542
20	51.0	2	0.126492	0.048216	21	803	60.49	25.83	0.422604
8	103.0	2	0.070612	0.035892	22	1985	52.18	17.04	0.289628
12	103.0	2	0.089408	0.042427	22	2052	53.18	20.33	0.344794
20	103.0	2	0.095123	0.043425	22	2137	51.94	21.25	0.235472
8	0.0	3	0.12865	0.079281	b			26.12	1.786684
8	0.0	3	0.133858	0.079281	t			26.81	1.908121
12	0.0	3	0.136525	0.098468	b			27.16	1.632455
12	0.0	3	0.152273	0.098468	t			29.14	1.953493
20	0.0	3	0.129794	0.120174	b			26.28	1.099628
20	0.0	3	0.141097	0.120174	t			27.75	1.262254

flow	label	rettime (s)	dst (dyn/cm)	2x rt kl	2x rt dst	area
8	11	4.907264	69.30	0.2669	69.30	38736.7
12	11	3.737492	70.13	0.3576	70.13	31872.6
20	11	4.161205	68.39	0.0890	66.27	67697.1
8	12	5.474137	64.42	0.2052	64.42	48704.4
12	12	4.484463	64.77	0.2393	64.77	47933.1
20	12	4.574927	63.61	0.0731	61.22	83386.7
8	21	3.775267	68.35	0.2778	68.35	21737.8
12	21	2.911508	69.32	0.3605	69.32	17702.9
20	21	2.458381	70.53	0.1422	67.04	19435.0
8	22	3.726525	62.16	0.2896	62.16	21109.8
12	22	3.123462	64.45	0.3447	64.45	20960.9
20	22	2.988235	63.94	0.1177	60.43	31414.4
8	b	2.431087				7558.76
8	t	2.368519				7077.70
12	b	2.337997				10275.0
12	t	2.179135				8586.42
20	b	2.416286				18616.3
20	t	2.288288				16217.8

1=tergitol
2=dss
3=cw

Appendix F

Data of Tergitol 200 mg/L Solutions

Data of Tergitol 200 mg/L Solutions

run	b/t	Kla	duNouy	X	inter
1090	b14	0.070782	51.53	2716	52.94
	t14	0.070782	52.08	2535	53.35
1091	b14	0.074134	51.21	2815	54.33
	t14	0.074313	50.52	2542	53.66
1092	b14	0.071933	51.79	2629	54.79
	t14	0.071933	52.05	2597	54.50
1093	b14	0.076398	52.54	2683	54.79
	t14	0.076398	51.86	2745	54.66
1094	b10	0.075512	53.36	2653	56.88
	t10	0.075512	52.64	2700	57.27
1095	b10	0.075391	53.29	2681	57.90
	t10	0.075391	52.87	2684	56.53
1096	b10	0.061984	53.23	3001	57.63
	t10	0.061984	53.32	2945	56.43
1097	b10	0.074257	53.98	2650	57.99
	t10	0.074257	53.69	2646	56.38
1098	t10	0.069918	53.91	3007	58.24
	b10	0.069918	53.78	2856	57.33
	m10	0.069918	53.95	2949	57.75
1099	t10	0.071046	54.44	2852	58.23
	b10	0.071046	54.24	2734	58.77
	m10	0.071046	45.23	2780	58.66
1102	t10	0.073922	51.60	2276	54.58
	b10	0.073922	51.80	2441	53.90
	m10	0.073922	52.32	2283	54.59
1103	t10	0.071923	52.20	2068	54.81
	b10	0.071923	52.20	2162	54.15
	m10	0.071923	52.20	2315	53.57
1104	t14	0.084063	53.30	2411	55.58
	b14	0.084063	53.00	3098	54.36
1105	t14	0.086827	53.30	2280	54.29
	b14	0.086827	53.30	2191	55.36
1106	t14	0.091826	53.40	2507	55.91
	b14	0.091826	54.20	2359	55.70
1107	b10	0.074399	54.43	2897	56.64
	t10	0.074399	54.10	2521	56.81
1108	b10	0.079326	54.40	2652	57.11
	t10	0.079326	53.70	2671	53.97

Data of Tergitol 200 mg/L Solutions

run	b/t	Kla	duNouy	X	inter
1113	b10	0.069576	51.86	2332	54.22
	t10	0.069576	52.18	2293	54.44
1114	b10	0.068913	51.30	2381	54.51
	t10	0.068913	51.27	2371	54.14
1115	b10	0.068972	52.73	2344	55.15
	t10	0.068972	51.95	1987	55.76
1116	b8		53.06	2474	56.11
	t8		53.16	2514	55.45
1117	b8	0.072517	53.59	2441	56.49
	t8	0.072517	52.73	2174	56.41
1118	b8	0.072303	53.58	2384	57.46
	t8	0.072303	53.32	2481	55.98
1119	b8	0.072136	53.71	2361	58.30
	t8	0.072136	53.49	2633	57.31
1120	b8	0.058266	54.01	2754	58.04
	t8	0.058266	54.11	2829	57.77
1121	b8	0.066301	54.24	2697	58.94
	t8	0.066301	53.81	2671	58.38
1122	b8	0.066494	54.37	3117	58.40
	t8	0.066494	53.87	3069	58.60
1123	b130	0.07094	54.37	2879	58.77
	t130	0.07094	53.64	2692	58.90
1124	b130	0.081248	55.02	2625	58.81
	t130	0.081248	54.53	2840	59.43
1125	b130	0.079311	53.84	2829	59.91
	t130	0.079311	55.19	2887	58.97
1126	b130	0.076977	56.23	2513	60.11
	t130	0.076977	55.38	2688	60.43
1127	b130	0.077504	56.23	2726	60.72
	t130	0.077504	56.27	2636	61.31
1128	b130	0.075412	56.66	2581	59.63
	t130	0.075412	56.43	2641	59.92
1129	b130	0.071476	56.27	2712	59.74
	t130	0.071476	56.43	2418	60.72

b = sample at bottom of tank
t = sample at top of tank
flow rate is after b/t
    130 = 20 L/min
    14 = 12 L/min
    10 = 8 L/min
    8 = 6 L/min

116

Appendix G

Solids and Conductivity Experiments

Solids and Conductivity Experiments

Test no	Conductivity (umhos)	#1 (mg/L)	#2 (mg/L)	#3 (mg/L)	ave (mg/L)
2001	468	430.4	429.2	420.0	426.5
2002	710	590.4	580.8	533.2	468.1
2003	860	672.0	652.8	675.2	666.7
2004	1120	838.0	842.8	794.8	825.2
2005	1260	984.0	980.8	950.4	971.7
2006	1470	1056.8	1044.4	1045.6	1048.9
2007	1620	1145.6	1199.2	1156.8	1167.2
2008	1730	1244.4	1336.0	1314.8	1298.4
2009	1960	1387.6	1430.4	1400.0	1406.0
2011	490	447.2	436.4	437.6	440.4
2012	730	608.0	555.6	588.0	583.9
2013	900	636.0	654.8	640.4	643.7
2014	1120	767.6	798.4	839.2	801.7
2015	1290	918.8	924.4	928.4	923.9
2016	1480	1100.4	1094.4	1040.8	1078.5
2017	1680	1240.4	1217.6	1165.6	1207.9
2018	1830	1315.2	1330.0	1327.6	1324.3
2019	2010	1467.2	1676.8	1488.3	1477.6
2020	465	368.8	352.8	395.6	372.4
2021	700	525.2	492.8	508.0	508.7
2022	890	660.8	644.0	615.6	640.1
2023	1050	807.2	795.6	786.0	796.3
2024	1230	939.6	938.0	927.2	934.9
2025	1500	1072.4	1074.8	1060.8	1069.3
2026	1650	1260.8	1258.0	1234.0	1250.9
2027	1800	1376.4	1410.0	1387.2	1391.2
2028	1980	1528.0	1501.6	1474.8	1501.5